

Emergent self-duality in long range critical spin chain: from deconfined criticality to first order transition

Sheng Yang,^{1,*} Zhiming Pan,^{2,*} Da-Chuan Lu,^{3,†} and Xue-Jia Yu^{4,5,‡}

¹*Zhejiang Institute of Modern Physics and School of Physics, Zhejiang University, Hangzhou 310027, China*

²*Institute for Theoretical Sciences, WestLake University, Hangzhou 310024, China*

³*Department of Physics, University of California, San Diego, CA 92093, USA*

⁴*Department of Physics, Fuzhou University, Fuzhou 350116, Fujian, China*

⁵*Fujian Key Laboratory of Quantum Information and Quantum Optics, College of Physics and Information Engineering, Fuzhou University, Fuzhou, Fujian 350108, China*

(Dated: September 15, 2024)

Over the past few decades, tremendous efforts have been devoted to understanding self-duality at the quantum critical point, which enlarges the global symmetry and constrains the dynamics. One-dimensional spin chain is an ideal platform for the theoretical investigation of these exotic phenomena, due to the powerful simulation method like density matrix renormalization group. Deconfined quantum criticality with self-duality at the critical point has been found in an extended short-range spin chain. In this work, we employ large-scale density matrix renormalization group simulations to investigate a critical spin chain with long-range power-law interaction $V(r) \sim 1/r^\alpha$. Remarkably, we reveal that the long-range interaction drives the original deconfined criticality towards a first-order phase transition as α decreases. More strikingly, the emergent self-duality leads to an enlarged symmetry and manifests at these first-order critical points. This discovery is reminiscent of self-duality protected multicritical points and provides the example of the critical line with generalized symmetry. Our work has far-reaching implications for ongoing experimental efforts in Rydberg atom quantum simulators.

I. INTRODUCTION

Quantum critical points (QCPs) and associated emergent phenomena in strongly correlated many-body systems stand as central topics within realms of both condensed matter and high-energy communities^{1–3}. A special property observed in certain QCPs is self-duality. Its origin can trace back to the Kramers-Wannier duality of the two-dimensional (2D) classical Ising model^{4,5} and has subsequently been established in a series of models featuring deconfined quantum critical points (DQCP)^{6–17}. More specifically, DQCP exhibits anomalies¹⁸, fractionalization¹⁹, self-duality^{12,20}, and emergent symmetry^{21–23}. Despite extensive theoretical^{12,16,24–39}, numerical^{40–75}, and experimental explorations^{76–78}, there is still ongoing efforts surrounding how exactly they have been implemented in lattice models and experimental setups.

Recently, quantum simulators like Rydberg atoms and ion traps have emerged as powerful tools for simulating exotic quantum phases and phase transitions^{79–89}. These systems offer intriguing opportunities for exploring long-range interactions in many-body systems, an area extensively investigated in condensed matter and ultracold atom physics^{90–97}. The critical behavior of long-range interacting systems has been widely studied in both quantum spin models^{98–112} and interacting fermion models^{113–116}. The presence of long-range interactions can effectively modify the system's dimensionality^{91,94,99,100,107}, leading to effects such as the breakdown of quantum-classical correspondence and the Mermin-Wagner theorem^{105,106,109,110}, thus can dramatically alter the phases and phase transitions. For instance, even in the case of conventional QCPs, the influence of long-range interactions generally gives rise to three distinct universality classes⁹¹: the mean-field universality class, the long-range “non-classical” universality class, and the short-range universality class. Certainly, a crucial question arises: How do long-range interac-

tions influence unconventional QCPs, like the DQCP? Does this interaction lead to new physical phenomena? Currently, these questions remain unanswered.

In this work, we address the fate of a 1D DQCP with long-range power-law decay interaction $V(r) \sim \frac{1}{r^\alpha}$, using both lattice simulations of a frustrated quantum spin model and renormalization group (RG) calculations of a proposed Luttinger-liquid field theory. Remarkably, we find there still exist DQCP and emergent symmetry for fast decay of the long-range interaction above a critical power $\alpha_c \approx 1.95$. This result is consistent with the predictions from bosonization and RG analyses. The most intriguing observation is that as the long-range interaction decays slower (i.e., $\alpha < \alpha_c$), the DQCP turns into a first-order phase transition with enlarged symmetry preserved by the emergent self-duality. This discovery goes beyond traditional understandings, particularly as emergent symmetry is generally associated with continuous QCPs. Our work clarifies and significantly extends the discussion of the DQCP phenomena in long-range interacting systems, and its signatures should be detectable in existing Rydberg atom experiments.

The rest of this paper is organized as follows: Sec. II presents the lattice model of the 1D DQCP with long-range power-law interaction and outlines the employed numerical method. Sections III and IV depict the phase diagram of the 1D DQCP with long-range interaction and the finite-size scaling of the critical behavior, along with an effective field theory to explain the aforementioned numerical results. The discussion and conclusion are presented in Sec. V. Additional data for our analytical and numerical calculations are provided in the Appendices.

II. MODEL AND METHOD

The system under study is a frustrated quantum spin chain proposed by Jiang and Motrunich (JM model)¹⁵, with addi-

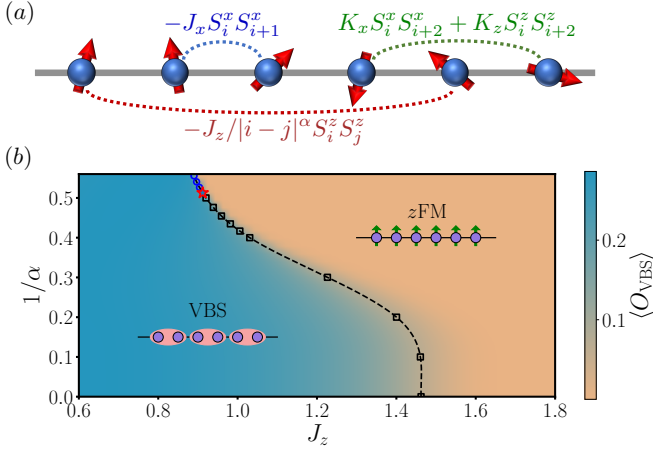


FIG. 1. (a) Schematic representation of the long-range JM model. (b) Phase diagram of the 1D spin Hamiltonian (1), mapped out by the VBS order parameter with $L = 128$. The markers obtained from the extrapolation of U_{zFM} crossing points demarcate the boundaries between the zFM and VBS ordered phases and the dashed line is a guide to the eye (see Figs. A1 and A3 for the details). The black squares indicate the continuous phase transition, while the blue circles indicate the first-order phase transition ($\alpha < \alpha_c$ with the estimated multicritical point $\alpha_c \approx 1.95$ marked by the red star).

tional long-range power-law interactions, depicted in Fig. 1(a). The model is defined by the following Hamiltonian:

$$H_{\text{LRJM}} = \sum_i (-J_x S_i^x S_{i+1}^x + K_x S_i^x S_{i+2}^x + K_z S_i^z S_{i+2}^z) - \frac{J_z}{N(\alpha)} \sum_{i < j} \frac{S_i^z S_j^z}{|i-j|^\alpha}, \quad (1)$$

where $S_i = (S_i^x, S_i^y, S_i^z)$ represents the spin-1/2 operator on each site i . J_γ/K_γ ($\gamma = x, z$) corresponds to the nearest/next-nearest neighbor ferromagnetic(FM)/antiferromagnetic(AFM) couplings. For simplicity, we set $K_x = K_z = 0.5$ and $J_x = 1.0$ as the energy unit below. The parameter α tunes the power of long-range $S^z - S^z$ interactions, which tends to the nearest-neighbor short-range JM model in the limit $\alpha \rightarrow \infty$. The Kac factor $N(\alpha) = \frac{1}{L-1} \sum_{i < j} \frac{1}{|i-j|^\alpha}$ is included to keep the Hamiltonian extensive.

When $\alpha \rightarrow \infty$, the original JM model exhibits a 1+1D analogy of DQCP^{15,117–119}. By tuning J_z , the system undergoes a continuous quantum phase transition between a valence-bond-solid (VBS) phase ($J_z \approx 1$) and a spin-ordered ferromagnetic (called zFM) phase ($J_z \gg 1$), which corresponds to the horizontal line $1/\alpha = 0$ in Fig. 1(b). The phase transition is analogous to the 2+1D DQCP⁸ as it represents a direct continuous transition between two incompatible spontaneous symmetry breaking phases^{15,117}. Moreover, it can be analytically described by a Luttinger-like field theory with central charge $c = 1$, featuring an emergent $O(2) \times O(2)$ symmetry at the deconfined critical point¹¹⁹.

To obtain the ground-state properties of the Hamiltonian H_{LRJM} , we adopt the density matrix renormalization group (DMRG)^{120–122} based on the matrix product state (MPS) tech-

nique^{122,123}, which has established itself as one of the best numerical approaches nowadays for one dimensional strongly-correlated systems. Our focus lies in exploring the resulting critical behaviors arising from the interplay between the DQCP and long-range interactions. For most of the calculations, we consider system sizes $L = 32$ –256, while for reliable finite-size scaling analyses, we simulate systems of size $L = 192$ –384. To guarantee the numerical accuracy and efficiency in practical calculations, we perform at most 50 DMRG sweeps with a gradually increased MPS bond dimension, $\chi \leq \chi_{\text{max}} = 2048$, under the open boundary condition. Once the MPS energy has converged up to the order 10^{-10} , the sweeping route would be stopped and the final MPS is believed to be a faithful representation of the true ground state.

III. NUMERICAL RESULTS

A. Quantum phase diagram: an overview

Before the illustration of the numerical results, we first summarize the main findings about the long-range JM model in Eq. (1). An accurate ground-state phase diagram expanded by the axes of $1/\alpha$ and J_z is displayed in Fig. 1(b). It is found that the long-range interaction physics can be classified into two distinct regimes separated by a critical power α_c . For $\alpha > \alpha_c$, the long-range power-law interaction decays very fast such that the interaction tail does not bring any essential change to the DQCP compared with the original model with nearest interaction. The VBS-to-zFM transition remains a direct continuous transition characterized by DQCP properties. This large α regime is in some sense roughly consistent with the classification given in Ref.⁹¹, which asserts that if α is larger than a certain critical value, the critical behavior should be indistinguishable from its short-range limit. However, the long-range interaction does extend the zFM phase region and the critical point shifts gradually towards smaller J_z with decreasing α as expected. Remarkably, what makes our results fundamentally different from the previous literature (see Ref.⁹¹ and references therein) is the small α regime. For the case of $\alpha < \alpha_c$, the phase transition is no longer continuous but is now driven into a first-order one by the sufficiently strong long-range interaction. More strikingly, our numerical calculations and low-energy field theory analysis consistently support that the self-duality emerged at the 1+1D DQCP is survived from the strong long-range interaction, giving rise to a first-order phase transition with an enlarged $O(2) \times O(2)$ symmetry, which is not well-studied in previous works.

B. Continuous phase transition at $\alpha > \alpha_c$

Similar to the case of conventional QCPs, it is found that the 1+1D analogy of the DQCP hosted in the original short-range JM model is robust against the long-range interaction when the power α is large enough.

To unveil the continuous nature of the transition, we calcu-

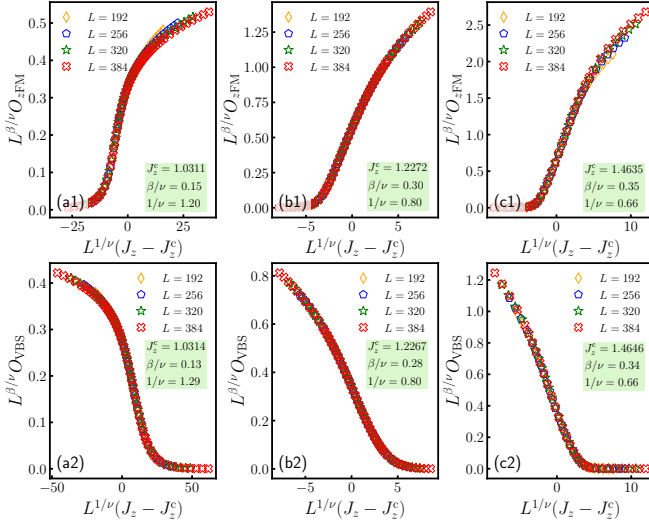


FIG. 2. The finite-size scaling analysis of order parameters O_{zFM} and O_{VBS} for the long-range JM model with $\alpha = 2.50$ [(a1)-(a2)], $\alpha = 3.33$ [(b1)-(b2)], and $\alpha = +\infty$ [(c1)-(c2)].

late the associated order parameters, respectively, given by

$$O_{zFM} = \frac{1}{L'} \sum_i S_i^z \text{ and } O_{VBS} = \frac{1}{L'} \sum_i (-1)^i S_i \cdot S_{i+1}, \quad (2)$$

where the summation is restricted within the middle $L' = L/2$ subsystem to reduce the boundary effect, and resort to standard finite-size scaling analyses according to the scaling form¹²⁴

$$\langle O_{zFM/VBS} \rangle = L^{-\beta/\nu} f[L^{1/\nu}(J_z - J_z^c)], \quad (3)$$

where β and ν are critical exponents of order parameter and correlation length, respectively. If the phase transition is continuous, the critical exponents extracted independently from the data collapses of O_{zFM} and O_{VBS} should be identical.

As elaborated in Fig. 2, we have performed conventional finite-size scaling analysis for several representative α values. It is noted that we have added a pinning field of strength 1 at both boundaries when we calculate the zFM order parameter, and we also further restrict the summation in Eq. (2) within the central two sites to minimize the boundary effect as we can. Similar to Ref.^{125,126}, we first adjust the exponent $\eta = \beta/\nu$ such that the curves $L^\eta \langle O_x \rangle$ as a function of J_z intersect with each other for all system sizes, and J_z^c can be estimated by the crossing point. Then we adjust the exponent $1/\nu$ until a good collapse of $L^\eta \langle O_x \rangle$ versus $L^{1/\nu}(J_z - J_z^c)$ for all L is achieved.

Following the detailed procedure, we present final data collapses of the order parameters in Fig. 2. It is evident that both order parameters obey the standard scaling relation (3) quite well and the extracted critical exponents β/ν are agreed with each other within numerical accuracy, corroborating that the 1+1D DQCP hosted in the original JM model is robust against the long-range S^z-S^z interaction when $\alpha > \alpha_c$. It is also interesting to notice that the exponents $\eta \equiv \beta/\nu$ and ν both decrease gradually as increasing $1/\alpha$, but the equality $2\nu(1-2\eta) = 1$ still holds roughly for all the α values examined here, which

is consistent with the prediction from the dual Luttinger-like theory calculations shown below.

C. First-order phase transition at $\alpha < \alpha_c$

Different from the large α regime, the VBS-to- zFM phase transition evolves from continuous to first order as the power α is decreased smaller than a certain critical value α_c , which is beyond the conventional classification of the critical behaviors affected by long-range interactions (see Sec. I or Ref.⁹¹).

A faithful quantity commonly used to distinguish between the continuous and first-order phase transitions is the Binder ratio U^{127} , which is defined by (for the zFM order here)

$$U_{zFM} = \frac{1}{2} \left(3 - \frac{\langle O_{zFM}^4 \rangle}{\langle O_{zFM}^2 \rangle^2} \right). \quad (4)$$

This observable has a vanishing scaling dimension and hence can give reliable information on the nature and position of the QCP. For continuous phase transitions, U_{zFM} typically shows a monotonic behavior, while for first-order phase transitions, U_{zFM} instead displays a nonmonotonic behavior and exhibits a diverged negative peak near the QCP with increasing system size¹²⁸⁻¹³⁰.

As shown in Fig. 3(a)-(b) and Fig. A1, it is found that there exists a critical value $\alpha_c \approx 1.95$, such that when $\alpha > \alpha_c$, the Binder ratio U_{zFM} shows a monotonic growth as J_z is increased, but when $\alpha < \alpha_c$, U_{zFM} exhibits a nonmonotonic behavior with J_z and develops a diverged negative peak near the transition point. The distinct behaviors of U_{zFM} imply that the quantum phase transition changes into a first-order type as α is decreased smaller than α_c . Furthermore, the precise critical point J_z^c can be determined by extrapolation based on the relation, $J_z^*(L) = J_z^c + aL^{-b}$, where $J_z^*(L)$ is the crossing point of $U_{zFM}(L)$ and $U_{zFM}(L+32)$ ¹²⁹. In Fig. 3(c)-(d), one can see a similar diverged negative peak developed in the VBS Binder ratio, $U_{VBS} = (3 - \langle O_{VBS}^4 \rangle / \langle O_{VBS}^2 \rangle^2)/2$, and the critical points obtained independently from U_{zFM} and U_{VBS} are close to each other. Other results of such least-squares fitting are included in Appendix C, and the estimated critical points are used to demarcate the phase boundaries in Fig. 1(b).

To further confirm the first-order phase transition happened at $\alpha < \alpha_c$, in Fig. 3(e), we also calculate the ground-state energy density e_g and its corresponding first derivative $\partial e_g / \partial J_z$ near the transition point for $\alpha = 1.8$. It is found that the first-derivative curves are more and more steep and a distinct jump is expected in the thermodynamic limit, which is a definite evidence for first-order phase transitions. Moreover, order parameters at their respective pseudocritical points $J_z^*(L)$ (i.e., crossing points of U_{zFM} and U_{VBS}) are displayed versus $1/L$ in Fig. 3(f). The coexistence of zFM and VBS orders at the critical point can be another decisive indicator of the first-order transition.

In summary, all the elaborated results consistently corroborate a first-order phase transition in the small α regime. As we have examined the observed phase transition from three different perspectives, each of which has been used as the main

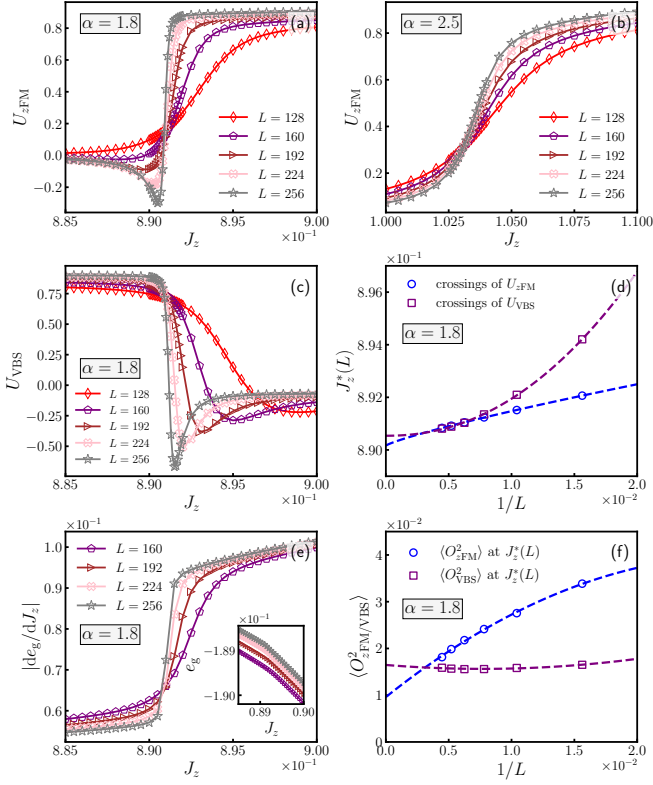


FIG. 3. (a)-(b) The Binder ratio of the magnetization $U_{z\text{FM}}$ versus J_z . (c) The Binder ratio of the VBS order U_{VBS} versus J_z . (d) The crossing points $J_z^*(L)$ of $U_x(L)$ and $U_x(L + 32)$ ($x = z\text{FM}$ or VBS) are displayed versus $1/L$. The dashed curves are least-squares fitting according to $J_z^*(L) = J_z^c + aL^{-b}$. (e) The ground-state energy per site and its first derivative with respect to J_z . (f) The squared order parameter $\langle O_x^2 \rangle$ ($x = z\text{FM}$ or VBS) at the finite-size pseudocritical points $J_z^*(L)$. The curves are second-order polynomial fits. (a) and (c-f) are plotted for $\alpha = 1.8$, but (b) is plotted for $\alpha = 2.5$.

evidence for first-order transitions in many works, the first-order transition found here should be reliable with these self-consistent results. It is also worth mentioning that a bimodal histogram of energy or certain quantities may give other evidence for the first-order transition, however, such an illustration seems not practicable within the adopted DMRG framework fundamentally distinct from the sampling-based Monte Carlo simulation. On the other hand, in the present work, we only focus on the properties of the first-order and continuous transitions. The tricritical point α_c is very interesting and can be studied by the flowgram method developed in¹³¹, but we leave it for future investigations.

D. Enlarged symmetry on the critical line

One of the most significant features of the 1+1D DQCP in the original short-range JM model is the $O(2) \times O(2)$ symmetry emerged exactly at the deconfined critical point^{15,117,119}. Therefore, it is natural to ask whether this enlarged symmetry still exists at the QCPs of the long-range JM model.

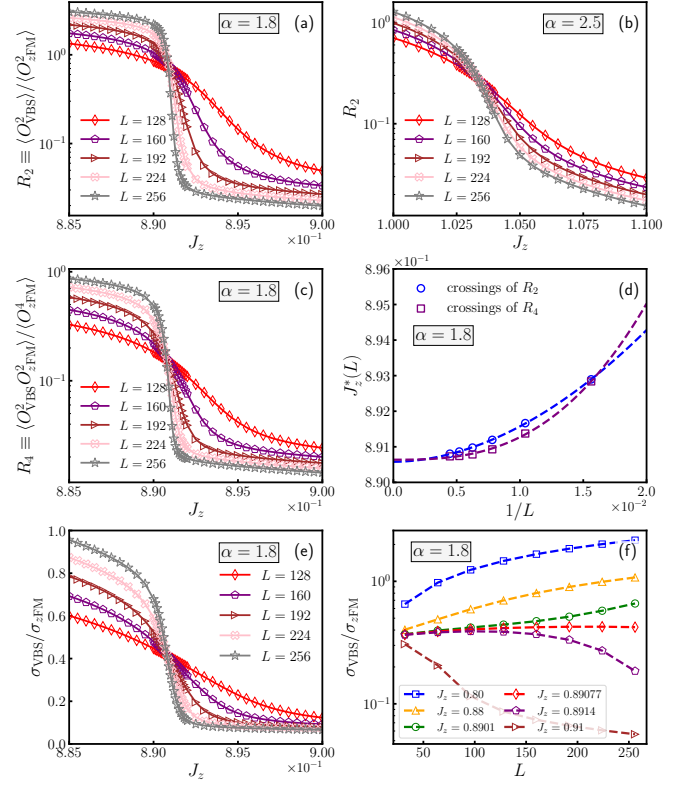


FIG. 4. (a)-(b) The ratio of the squared order parameters R_2 versus J_z . (c) The cross ratio of the squared order parameters R_4 versus J_z . (d) The crossing locations $J_z^*(L)$ of $R_{2/4}(L)$ and $R_{2/4}(L + 32)$ are shown versus $1/L$. The dashed curves are least-squares fitting according to the relation, $J_z^*(L) = J_z^c + aL^{-b}$. (e) The variance ratio $\sigma_{\text{VBS}} / \sigma_{z\text{FM}}$, where $\sigma_x \equiv (\langle O_x^4 \rangle - \langle O_x^2 \rangle^2)^{1/2}$ ($x = z\text{FM}$ or VBS), as a function of J_z for several system sizes. (f) The ratio $\sigma_{\text{VBS}} / \sigma_{z\text{FM}}$ as a function of L for several J_z near the critical point J_z^c . (a) and (c-f) are plotted for $\alpha = 1.8$, but (b) is plotted for $\alpha = 2.5$.

For this purpose, we calculate the ratio of the squared order parameters defined by $R_2 = \langle O_{\text{VBS}}^2 \rangle / \langle O_{z\text{FM}}^2 \rangle$. According to Refs.^{22,59,132,133}, if the VBS and $z\text{FM}$ order parameters have the same scaling dimension, the ratio R_2 should be size-independent at the transition point, and the QCP would have an enlarged symmetry that rotates these two orders. The results of R_2 are detailed and summarized in Fig. 4(a)-(b) and Fig. A2; it is obvious that R_2 becomes size-independent near the QCP for all α , indicating that the VBS-to- $z\text{FM}$ transition still hosts the $O(2) \times O(2)$ symmetry even when its nature has been driven into first-order. Similarly, as shown in Fig. 4(c)-(d), the cross ratio of order parameters, $R_4 = \langle O_{\text{VBS}}^2 O_{z\text{FM}}^2 \rangle / \langle O_{z\text{FM}}^4 \rangle$, of different system sizes also intersect with each other roughly at a single point, and the extrapolation of the pseudocritical point is also close to the one obtained from the ratio R_2 .

In Fig. 4(e), we also examine the variance ratio $\sigma_{\text{VBS}} / \sigma_{z\text{FM}}$ where $\sigma_x \equiv (\langle O_x^4 \rangle - \langle O_x^2 \rangle^2)^{1/2}$ ^{22,134}, which is another useful detector for symmetries at QCPs. Similar to R_2 , we can indeed see an intersection of $\sigma_{\text{VBS}} / \sigma_{z\text{FM}}$ curves of all L at the transition point. Fig. 4(f) explicitly shows the dependence of $\sigma_{\text{VBS}} / \sigma_{z\text{FM}}$ on L near the critical point. The universal behav-

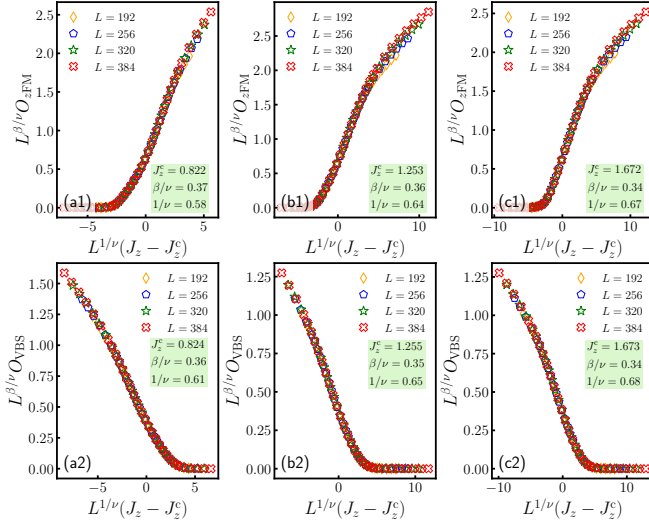


FIG. 5. The finite-size scaling analysis of order parameters O_{zFM} and O_{VBS} for the original JM model with $K_z = 0.2$ [(a1)-(a2)], $K_z = 0.4$ [(b1)-(b2)], and $K_z = 0.6$ [(c1)-(c2)].

ior of $\sigma_{VBS}/\sigma_{zFM}$ around $J_z \approx 0.8908$ gives another evidence for the enlarged $O(2) \times O(2)$ symmetry at the first-order phase transition.

Till now, the presented numerical simulations are consistent with each other and points to a first-order phase transition with enlarged $O(2) \times O(2)$ symmetry beyond conventional understandings. Therefore, it is necessary to explain our results, and the key point is the emergent self-duality survived from the long-range interaction which preserves the $O(2) \times O(2)$ symmetry.

E. Transition nature of the original JM model with $K_z \neq 1/2$

Before the presentation of the low-energy field theory analysis, it is also necessary to verify that the observed first-order phase transition is not induced by the naive modification of K_z , since the inclusion of the long-range $S^z - S^z$ interaction in the JM model can effectively change the value of K_z . For this purpose, we investigate the quantum phase transition of the *original* JM model with the parameter setting, $J_x = 1$, $K_x = 1/2$, and $K_z \neq 1/2$.

Following the same procedure explained in Sec. III B, we utilize the standard finite-size scaling analysis according to Eq. (3) to extract the quantum critical point J_z^c and related critical exponents, β and ν . As summarized in Fig. 5, it is clear that the obtained critical exponents β/ν are almost identical for zFM and VBS orders, which is a key property of the DQCP theory¹⁵, indicating that the quantum phase transition is still continuous. As the effective value of K_z modified by the long-range $S^z - S^z$ interaction, $K_z^{\text{eff}} = 1/2 - J_z/[2^\alpha N(\alpha)]$, is larger than 0.2 at the critical point for $\alpha = 1.8$, the results shown here can support that the first-order phase transition found in the long-range JM model at $\alpha = 1.8$ is indeed induced by the long-range $S^z - S^z$ interaction, thus ruling out the possibility

that the first-order transition is caused by a naive modification of the coupling K_z in the original JM model.

IV. LOW-ENERGY EFFECTIVE THEORY

The phase transition between the zFM and VBS orders is second order when α is large and first order when α is small. The continuous to first order transition happens at the critical power α_c . This continuous to first-order transition is driven by the long-range $S^z - S^z$ interaction. According to the bosonization method^{15,118,135} (see Section A of Appendix for the details), the spin operators can be represented by a bosonic field ϕ in the continuous limit,

$$S_j^z \sim \cos \phi(x)/2, \quad S_j^x \sim -\sin \phi(x)/2, \quad (5)$$

where the discrete coordinate is replaced by its continuous version, $x_j \rightarrow x$. Thus, the 1D long-range $S^z - S^z$ interaction takes the following form in the effective continuum theory¹⁰⁹,

$$\sum_{i,j} \frac{S_i^z S_j^z}{|i-j|^\alpha} \sim \int dx dy \frac{\cos[\phi(x)] \cos[\phi(y)]}{4|x-y|^\alpha}, \quad (6)$$

where x, y are the 1D continuous coordinates. The effective action in the Euclidean path integral formulation under bosonization is given by^{15,135},

$$S = \int d\tau dx \left[\frac{i}{\pi} \partial_\tau \phi \partial_x \theta + \frac{v}{2\pi} \left(\frac{1}{g} (\partial_x \theta)^2 + g (\partial_x \phi)^2 \right) \right] + \int d\tau dx \left[\lambda_u \cos(4\theta) + \lambda_a \cos(2\phi) \right] + S_{LR}. \quad (7)$$

with imaginary time τ , spatial coordinates x , velocity v and Luttinger parameter g . λ_u and λ_a are the most relevant short-range interaction which persevering the symmetry of the JM model. The long-range part in the Lagrangian is deduced from Eq. (6),

$$S_{LR} = \frac{\lambda_+}{2} \int d\tau dx dr \frac{1}{|r|^\alpha} \cos[\phi(x+r, \tau) + \phi(x, \tau)] + \frac{\lambda_-}{2} \int d\tau dx dr \frac{1}{|r|^\alpha} \cos[\phi(x+r, \tau) - \phi(x, \tau)]. \quad (8)$$

where r denotes the relative distance of the fields. Here, the cos-cos correlation in Eq. (6) has been separated into two parts, whose effects would be different. For smaller interaction range r , λ_- will contribute to the renormalization of the Luttinger parameters. We would focus on the renormalization of the long-range contribution and can omit this shorter range r contribution at this stage. Moreover, it should also be noticed that the Luttinger parameter g could be a non-universal quantity at the critical point. While for the pure XXZ model, the explicit value of g could be deduced from the microscopic parameters based on the Bethe ansatz^{136–138}, for the general spin model, e.g., for the JM model with long-range interaction, it would be hard to handle out the explicit value of g from the microscopic parameters.

Based on the RG analysis (in Section B of Appendix), the long-range S^z - S^z interaction Eq. (8) is irrelevant or less relevant than the short-range one when the exponent is greater than some critical value, $\alpha > \alpha_c$. In the large α regime, the continuous transition between the VBS and zFM phases driven by short-range interaction¹⁵ is stable against the long-range perturbation. On the other hand, when α is smaller than the critical value, the long-range S^z - S^z interaction becomes the most relevant operator of the system and drives the continuous transition to a first order transition. To decode the non-trivial transition between the VBS and zFM phases, it will be more sufficient to work in the effective dual theory formulation, as done in the original JM model^{15,117–119}.

A. Dual field theory

The dual field theory description plays important role for understanding the 1D DQCP nature of the JM model¹⁵. Especially, the continuous transition between VBS and zFM phases in the original JM model has emergent self-duality as shown in^{15,117–119}, since the scaling dimensions of the two order parameters are the same in both numerical and theoretical calculations. While the construction of the dual theory field requires much effort, the final formulation is direct and simple, that is, the z-FM and VBS order parameters could be represented by the continuous dual field $\tilde{\theta}$ as $\Psi_{\text{zFM}} \sim \sin(\tilde{\theta})$ and $\Psi_{\text{VBS}} \sim \cos(\tilde{\theta})$ ¹⁵. The dual field theory unifies zFM and VBS order parameters together by the single field $\tilde{\theta}$. The self-duality manifests in the dual Luttinger liquid theory in the imaginary-time path integral action^{15,135},

$$\tilde{S} = \int d\tau dx \left[\frac{i}{\pi} \partial_\tau \tilde{\theta} \partial_x \tilde{\theta} + \frac{\tilde{v}}{2\pi} \left(\frac{1}{\tilde{g}} (\partial_x \tilde{\theta})^2 + \tilde{g} (\partial_x \tilde{\phi})^2 \right) \right] + \int d\tau dx \left[\tilde{\lambda} \cos(2\tilde{\theta}) \right] + \tilde{S}_{LR}, \quad (9)$$

with the (1 + 1)D spatial-time coordinates (x, τ) , effective velocity \tilde{v} and Luttinger parameter \tilde{g} . The tilde symbol is used to emphasize the difference from the original field theory in Eq. (9). $(\tilde{\theta}, \tilde{\phi})$ is a pair of conjugate fields in the dual field theory¹⁵. We first summarized some basic results in the short range system without \tilde{S}_{LR} ^{15,117–119}. Since the relevant problem lying in the parameter regime $\tilde{g} \in (1/2, 2)$, $\tilde{\lambda}$ is the only relevant short-ranged operator, which could drive the phase transition between the z-FM and VBS orders. A relevant positive (negative) $\tilde{\lambda}$ will pin down the dual field $\tilde{\theta} = \frac{\pi}{2}$ ($\tilde{\theta} = 0$), which corresponds to the zFM (VBS) phase, $\Psi_{\text{zFM}} \neq 0$ ($\Psi_{\text{VBS}} \neq 0$). On the contrary, $\tilde{\phi}$ field could be fully integrated out in the path integral since its interaction term is irrelevant in the critical theory, leading to a pure sine-Gordon theory for the field $\tilde{\theta}$. Instantly, zFM and VBS order parameters have the same scaling dimensions $\dim[\Psi_{\text{zFM}}] = \dim[\Psi_{\text{VBS}}] = \tilde{g}/4$ ^{15,117}. The emergent self-duality permutes VBS and zFM order parameters. Combined with the global symmetry $O(2)$, the emergent self-duality promotes the global symmetry to $O(2) \times O(2)$.

From the above numerical simulations, the substantial evidence shows that the emergent self-duality still persists in the

first order transition when the long-range S^z - S^z interaction is relevant. Indeed, the long-range S^z - S^z interaction is effectively self-dual preserving at the critical point. Based on the dual Bosonization approach, the long-range S^z - S^z interaction in the dual theory is represented as,

$$\tilde{S}_{LR} = \frac{\tilde{\lambda}_-}{2} \int d\tau dx dr \frac{1}{|r|^\alpha} \cos [\tilde{\theta}(x+r, \tau) - \tilde{\theta}(x, \tau)] - \frac{\tilde{\lambda}_+}{2} \int d\tau dx dr \frac{1}{|r|^\alpha} \cos [\tilde{\theta}(x+r, \tau) + \tilde{\theta}(x, \tau)]. \quad (10)$$

Here, the effective coupling $\tilde{\lambda}_-$ drives the system to a spatial uniform pattern, while the sign of $\tilde{\lambda}_+$ leads to the VBS or zFM order. In the infrared limit, long-range $\tilde{\lambda}_+$ has a similar effect as the short-range $\tilde{\lambda}$ and a combination of them leads to an renormalized driving coupling, which will tune the phase transition between VBS and zFM order. This effective tuning coupling also accounts for the shift of the phase boundary to the left in Fig. 1 (b). Under the RG flow (in Section B of SM), $\tilde{\lambda}_-$ becomes more relevant than $\tilde{\lambda}_+$, while the VBS-zFM phase transition is still tuned by $\tilde{\lambda}_+$. When the power of long-range interaction becomes smaller than the critical value $\alpha < \alpha_c$, $\tilde{\lambda}_-$ becomes the most relevant operator of the system, driving the second order transition into a first order one. Therefore, only $\tilde{\lambda}_-$ term affects the infrared fate along the critical line.

Under the self-duality $\sin(\tilde{\theta}) \leftrightarrow \cos(\tilde{\theta})$, the long-range interaction transforms as $\tilde{\lambda}_- \rightarrow \tilde{\lambda}_-, \tilde{\lambda}_+ \rightarrow -\tilde{\lambda}_+$. The $\tilde{\lambda}_-$ term is manifestly self-dual invariant. On the contrary, the $\tilde{\lambda}_+$ term breaks the self-duality and transforms the same as $\tilde{\lambda}$. Along the critical line, the VBS to zFM tuning coupling tends to zero and the system is self-dual invariant in the low-energy field theory. The emergent self-duality persists along the transition line from continuous to first order transition. This can be understood as the self-duality protected criticality¹³⁹. Since the self-duality permutes the two phases VBS and zFM, the self-duality invariant region should be the interface between them, and that is the phase boundary in Fig. 1 (b).

V. DISCUSSIONS AND CONCLUSIONS

We noticed that some researchers have discovered emergent symmetry at special^{140,141} or weakly first-order transitions^{142–145}. They explained that the absence of a free energy barrier allows different orders to transform into each other. However, we emphasize that our model exhibits an unambiguous enlarged $O(2) \times O(2)$ symmetry at the strong first-order phase transition, which is different from the previous cases. Our findings reveal that, in the low-energy effective field theory, the self-dual invariant long-range operator changes from being irrelevant to relevant as α decreases, resulting in a first-order critical point with emergent self-duality, which leads to enlarged $O(2) \times O(2)$ global symmetry. Additionally, emergent supersymmetry¹⁴⁶ has also been discovered at first-order critical points.

Regarding experimental realization, Lee et al¹⁴⁷ recently proposed a Landau-forbidden quantum phase transition with an emergent symmetry in a one-dimensional strongly interacting array of trapped neutral Rydberg atoms. This can be

experimentally observed with measurement snapshots on a standard computational basis.

In conclusion, we perform large-scale DMRG simulations to decipher the critical properties of the JM model with long-range interactions. Our numerical simulation unambiguously demonstrates that the emergent self-duality appears along the critical line, from the continuous transition to the first-order transition. And the self-duality enlarges the global symmetry to $O(2) \times O(2)$. This finding aligns with the Luttinger-liquid theory calculations, where part of the long-range spin-spin interaction becomes the self-dual invariant relevant operator and drives the continuous transition to the first order transition. This is reminiscent of the tricritical Ising model, where the self-dual invariant operator can drive the tricritical point to either the Ising transition or the first order transition. In particular, the first order transition is a gapped phase with 3 groundstate degeneracies due to the anomalous self-duality^{148,149}.

We leave for future work the determination of a precise value

of α_c , comparisons of universal quantities with long-range interactions through renormalization group analysis, and a comparative study of the quantum critical behavior at the multicritical point. Our work paves a new way for understanding the interplay between unconventional quantum critical points and long-range physics through experimental and theoretically controlled manner.

ACKNOWLEDGMENTS

We thanks Yi-Zhuang You, Zi Yang Meng, Ruben Verresen, and Hai-Qing Lin for very helpful discussions. Numerical simulations were carried out with the ITENSOR package¹⁵⁰ on the Kirin No.2 High Performance Cluster supported by the Institute for Fusion Theory and Simulation (IFTS) at Zhejiang University. Z.P. is supported by National Natural Science Foundation of China (No. 12147104). X.-J. Yu acknowledges support from the start-up grant of Fuzhou University.

* The first two authors contributed equally.

† dclu137@gmail.com

‡ xuejiayu@fzu.edu.cn

- ¹ Subir Sachdev, *Quantum Phases of Matter* (Cambridge University Press, 2023).
- ² Subir Sachdev, *Quantum Phase Transitions*, 2nd ed. (Cambridge University Press, 2011).
- ³ Kenneth G. Wilson, “The renormalization group and critical phenomena,” *Rev. Mod. Phys.* **55**, 583–600 (1983).
- ⁴ H. A. Kramers and G. H. Wannier, “Statistics of the two-dimensional ferromagnet. part i,” *Phys. Rev.* **60**, 252–262 (1941).
- ⁵ Leo P. Kadanoff and Horacio Ceva, “Determination of an operator algebra for the two-dimensional ising model,” *Phys. Rev. B* **3**, 3918–3939 (1971).
- ⁶ Cenke Xu, “Unconventional quantum critical points,” *International Journal of Modern Physics B* **26**, 1230007 (2012).
- ⁷ T. Senthil, Leon Balents, Subir Sachdev, Ashvin Vishwanath, and Matthew P. A. Fisher, “Quantum criticality beyond the landau-ginzburg-wilson paradigm,” *Phys. Rev. B* **70**, 144407 (2004).
- ⁸ Todadri Senthil, Leon Balents, Subir Sachdev, Ashvin Vishwanath, and Matthew P. A. Fisher, “Deconfined criticality critically defined,” *Journal of the Physical Society of Japan* **74**, 1–9 (2005).
- ⁹ Michael Levin and T. Senthil, “Deconfined quantum criticality and néel order via dimer disorder,” *Phys. Rev. B* **70**, 220403 (2004).
- ¹⁰ T. Senthil and Matthew P. A. Fisher, “Competing orders, nonlinear sigma models, and topological terms in quantum magnets,” *Phys. Rev. B* **74**, 064405 (2006).
- ¹¹ Brian Swingle and T. Senthil, “Structure of entanglement at deconfined quantum critical points,” *Phys. Rev. B* **86**, 155131 (2012).
- ¹² Chong Wang, Adam Nahum, Max A. Metlitski, Cenke Xu, and T. Senthil, “Deconfined quantum critical points: Symmetries and dualities,” *Phys. Rev. X* **7**, 031051 (2017).
- ¹³ Zhen Bi and T. Senthil, “Adventure in topological phase transitions in 3 + 1-d: Non-abelian deconfined quantum criticalities and a possible duality,” *Phys. Rev. X* **9**, 021034 (2019).
- ¹⁴ Zhen Bi, Ethan Lake, and T. Senthil, “Landau ordering phase transitions beyond the landau paradigm,” *Phys. Rev. Res.* **2**, 023031 (2020).
- ¹⁵ Shenghan Jiang and Olexei Motrunich, “Ising ferromagnet to valence bond solid transition in a one-dimensional spin chain: Analogies to deconfined quantum critical points,” *Physical Review B* **99**, 075103 (2019).
- ¹⁶ T. Senthil, “Deconfined quantum critical points: a review,” (2023), [arXiv:2306.12638 \[cond-mat.str-el\]](https://arxiv.org/abs/2306.12638).
- ¹⁷ Ömer M. Aksoy, Christopher Mudry, Akira Furusaki, and Apoorv Tiwari, “Lieb-schultz-mattis anomalies and web of dualities induced by gauging in quantum spin chains,” (2023), [arXiv:2308.00743 \[cond-mat.str-el\]](https://arxiv.org/abs/2308.00743).
- ¹⁸ Max A. Metlitski and Ryan Thorngren, “Intrinsic and emergent anomalies at deconfined critical points,” *Phys. Rev. B* **98**, 085140 (2018).
- ¹⁹ Nvsen Ma, Guang-Yu Sun, Yi-Zhuang You, Cenke Xu, Ashvin Vishwanath, Anders W. Sandvik, and Zi Yang Meng, “Dynamical signature of fractionalization at a deconfined quantum critical point,” *Phys. Rev. B* **98**, 174421 (2018).
- ²⁰ Yan Qi Qin, Yuan-Yao He, Yi-Zhuang You, Zhong-Yi Lu, Arnab Sen, Anders W. Sandvik, Cenke Xu, and Zi Yang Meng, “Duality between the deconfined quantum-critical point and the bosonic topological transition,” *Phys. Rev. X* **7**, 031052 (2017).
- ²¹ Anders W. Sandvik, “Evidence for deconfined quantum criticality in a two-dimensional heisenberg model with four-spin interactions,” *Phys. Rev. Lett.* **98**, 227202 (2007).
- ²² Adam Nahum, P. Serna, J. T. Chalker, M. Ortuño, and A. M. Somoza, “Emergent $so(5)$ symmetry at the néel to valence-bond-solid transition,” *Phys. Rev. Lett.* **115**, 267203 (2015).
- ²³ Nvsen Ma, Yi-Zhuang You, and Zi Yang Meng, “Role of noether’s theorem at the deconfined quantum critical point,” *Phys. Rev. Lett.* **122**, 175701 (2019).
- ²⁴ Ruochen Ma and Chong Wang, “Theory of deconfined pseudo-criticality,” *Phys. Rev. B* **102**, 020407 (2020).
- ²⁵ Adam Nahum, “Note on wess-zumino-witten models and quasiuniversality in 2 + 1 dimensions,” *Phys. Rev. B* **102**, 201116 (2020).
- ²⁶ Da-Chuan Lu, “Nonlinear sigma model description of deconfined quantum criticality in arbitrary dimensions,” (2022),

- arXiv:2209.00670 [cond-mat.str-el].
- 27 Wenjie Ji, Nathanan Tantivasadakarn, and Cenke Xu, “Boundary states of three dimensional topological order and the deconfined quantum critical point,” (2022), arXiv:2212.09754 [cond-mat.str-el].
 - 28 Saranesh Prembabu, Ryan Thorngren, and Ruben Verresen, “Boundary deconfined quantum criticality at transitions between symmetry-protected topological chains,” (2022), arXiv:2208.12258 [cond-mat.str-el].
 - 29 Carolyn Zhang and Michael Levin, “Exactly solvable model for a deconfined quantum critical point in 1d,” *Phys. Rev. Lett.* **130**, 026801 (2023).
 - 30 Vira Shyt, Jeroen van den Brink, and Flavio S. Nogueira, “Frozen deconfined quantum criticality,” *Phys. Rev. Lett.* **129**, 227203 (2022).
 - 31 Darshan G. Joshi, Chenyuan Li, Grigory Tarnopolsky, Antoine Georges, and Subir Sachdev, “Deconfined critical point in a doped random quantum heisenberg magnet,” *Phys. Rev. X* **10**, 021033 (2020).
 - 32 Jong Yeon Lee, Yi-Zhuang You, Subir Sachdev, and Ashvin Vishwanath, “Signatures of a deconfined phase transition on the shastry-sutherland lattice: Applications to quantum critical $\text{SrCu}_2(\text{BO}_3)_2$,” *Phys. Rev. X* **9**, 041037 (2019).
 - 33 Yi-Zhuang You, Yin-Chen He, Cenke Xu, and Ashvin Vishwanath, “Symmetric fermion mass generation as deconfined quantum criticality,” *Phys. Rev. X* **8**, 011026 (2018).
 - 34 Chao-Ming Jian, Alex Thomson, Alex Rasmussen, Zhen Bi, and Cenke Xu, “Deconfined quantum critical point on the triangular lattice,” *Phys. Rev. B* **97**, 195115 (2018).
 - 35 Chao-Ming Jian, Alex Rasmussen, Yi-Zhuang You, and Cenke Xu, “Emergent symmetry and tricritical points near the deconfined quantum critical point,” (2017), arXiv:1708.03050 [cond-mat.str-el].
 - 36 Liujun Zou, Yin-Chen He, and Chong Wang, “Stiefel liquids: Possible non-lagrangian quantum criticality from intertwined orders,” *Phys. Rev. X* **11**, 031043 (2021).
 - 37 Xue-Yang Song, Chong Wang, Ashvin Vishwanath, and Yin-Chen He, “Unifying description of competing orders in two-dimensional quantum magnets,” *Nature communications* **10**, 4254 (2019).
 - 38 Xue-Yang Song, Yin-Chen He, Ashvin Vishwanath, and Chong Wang, “From spinon band topology to the symmetry quantum numbers of monopoles in dirac spin liquids,” *Phys. Rev. X* **10**, 011033 (2020).
 - 39 Lukas Janssen and Yin-Chen He, “Critical behavior of the qcd_3 -gross-neveu model: Duality and deconfined criticality,” *Phys. Rev. B* **96**, 205113 (2017).
 - 40 Anders W. Sandvik, “Continuous quantum phase transition between an antiferromagnet and a valence-bond solid in two dimensions: Evidence for logarithmic corrections to scaling,” *Phys. Rev. Lett.* **104**, 177201 (2010).
 - 41 Ribhu K. Kaul and Anders W. Sandvik, “Lattice model for the $\text{SU}(n)$ n el to valence-bond solid quantum phase transition at large n ,” *Phys. Rev. Lett.* **108**, 137201 (2012).
 - 42 Anders W. Sandvik and Bowen Zhao, “Consistent scaling exponents at the deconfined quantum-critical point*,” *Chinese Physics Letters* **37**, 057502 (2020).
 - 43 Hui Shao, Wenan Guo, and Anders W Sandvik, “Quantum criticality with two length scales,” *Science* **352**, 213–216 (2016).
 - 44 Matthew S. Block, Roger G. Melko, and Ribhu K. Kaul, “Fate of $\mathbb{C}l^{N-1}$ fixed points with q monopoles,” *Phys. Rev. Lett.* **111**, 137202 (2013).
 - 45 Ribhu K. Kaul and Roger G. Melko, “Large- n estimates of universal amplitudes of the $\mathbb{C}l^{N-1}$ theory and comparison with a $s = \frac{1}{2}$ square-lattice model with competing four-spin interactions,” *Phys. Rev. B* **78**, 014417 (2008).
 - 46 Yu Nakayama and Tomoki Ohtsuki, “Necessary condition for emergent symmetry from the conformal bootstrap,” *Phys. Rev. Lett.* **117**, 131601 (2016).
 - 47 Yin-Chen He, Junchen Rong, and Ning Su, “Non-Wilson-Fisher kinks of $O(N)$ numerical bootstrap: from the deconfined phase transition to a putative new family of CFTs,” *SciPost Phys.* **10**, 115 (2021).
 - 48 Yu-Rong Shu, Shao-Kai Jian, Anders W. Sandvik, and Shuai Yin, “Equilibration of topological defects at the deconfined quantum critical point,” (2023), arXiv:2305.04771 [cond-mat.str-el].
 - 49 Zi-Xiang Li, Shao-Kai Jian, and Hong Yao, “Deconfined quantum criticality and emergent $\text{so}(5)$ symmetry in fermionic systems,” (2019), arXiv:1904.10975 [cond-mat.str-el].
 - 50 Dong-Xu Liu, Zijian Xiong, Yining Xu, and Xue-Feng Zhang, “Does deconfined quantum phase transition have to keep lorentz symmetry? two velocities of spinon and string,” (2023), arXiv:2301.12864 [cond-mat.str-el].
 - 51 Xue-Feng Zhang, Yin-Chen He, Sebastian Eggert, Roderich Moessner, and Frank Pollmann, “Continuous easy-plane deconfined phase transition on the kagome lattice,” *Phys. Rev. Lett.* **120**, 115702 (2018).
 - 52 Bin-Bin Chen, Xu Zhang, Yuxuan Wang, Kai Sun, and Zi Yang Meng, “Phases of $(2+1)\text{d}$ $\text{so}(5)$ non-linear sigma model with a topological term on a sphere: multicritical point and disorder phase,” (2023), arXiv:2307.05307 [cond-mat.str-el].
 - 53 Menghan Song, Jiarui Zhao, Lukas Janssen, Michael M. Scherer, and Zi Yang Meng, “Deconfined quantum criticality lost,” (2023), arXiv:2307.02547 [cond-mat.str-el].
 - 54 Zi Hong Liu, Weilun Jiang, Bin-Bin Chen, Junchen Rong, Meng Cheng, Kai Sun, Zi Yang Meng, and Fakher F. Assaad, “Fermion disorder operator at gross-neveu and deconfined quantum criticalities,” *Phys. Rev. Lett.* **130**, 266501 (2023).
 - 55 Yuan Da Liao, Xiao Yan Xu, Zi Yang Meng, and Yang Qi, “Dirac fermions with plaquette interactions. i. $\text{su}(2)$ phase diagram with gross-neveu and deconfined quantum criticalities,” *Phys. Rev. B* **106**, 075111 (2022).
 - 56 Jiarui Zhao, Yan-Cheng Wang, Zheng Yan, Meng Cheng, and Zi Yang Meng, “Scaling of entanglement entropy at deconfined quantum criticality,” *Phys. Rev. Lett.* **128**, 010601 (2022).
 - 57 Yan-Cheng Wang, Nvsen Ma, Meng Cheng, and Zi Yang Meng, “Scaling of the disorder operator at deconfined quantum criticality,” *SciPost Phys.* **13**, 123 (2022).
 - 58 Yuan Da Liao, Gaopei Pan, Weilun Jiang, Yang Qi, and Zi Yang Meng, “The teaching from entanglement: 2d $\text{su}(2)$ antiferromagnet to valence bond solid deconfined quantum critical points are not conformal,” (2023), arXiv:2302.11742 [cond-mat.str-el].
 - 59 Wen-Yuan Liu, Shou-Shu Gong, Wei-Qiang Chen, and Zheng-Cheng Gu, “Emergent symmetry in frustrated magnets: From deconfined quantum critical point to gapless quantum spin liquid,” (2022), arXiv:2212.00707 [cond-mat.str-el].
 - 60 Yi-Zhuang You and Juven Wang, “Deconfined quantum criticality among grant unified theories,” *A Festschrift in Honor of the CN Yang Centenary: Scientific Papers*, 367–383 (2022).
 - 61 Ning Xi and Rong Yu, “Dynamical signatures of the one-dimensional deconfined quantum critical point,” *Chinese Physics B* **31**, 057501 (2022).
 - 62 Yu-Rong Shu and Shuai Yin, “Dual dynamic scaling in deconfined quantum criticality,” *Phys. Rev. B* **105**, 104420 (2022).
 - 63 Wen-Yuan Liu, Juraj Hasik, Shou-Shu Gong, Didier Poilblanc, Wei-Qiang Chen, and Zheng-Cheng Gu, “Emergence of gapless quantum spin liquid from deconfined quantum critical point,” *Phys. Rev. X* **12**, 031039 (2022).

- 64 Zi Hong Liu, Matthias Vojta, Fakher F. Assaad, and Lukas Janssen, “Metallic and deconfined quantum criticality in dirac systems,” *Phys. Rev. Lett.* **128**, 087201 (2022).
- 65 Yu-Rong Shu, Shao-Kai Jian, and Shuai Yin, “Nonequilibrium dynamics of deconfined quantum critical point in imaginary time,” *Phys. Rev. Lett.* **128**, 020601 (2022).
- 66 Rui-Zhen Huang and Shuai Yin, “Kibble-zurek mechanism for a one-dimensional incarnation of a deconfined quantum critical point,” *Phys. Rev. Res.* **2**, 023175 (2020).
- 67 Tian-Sheng Zeng, D. N. Sheng, and W. Zhu, “Continuous phase transition between bosonic integer quantum hall liquid and a trivial insulator: Evidence for deconfined quantum criticality,” *Phys. Rev. B* **101**, 035138 (2020).
- 68 Gaoyong Sun, Bo-Bo Wei, and Su-Peng Kou, “Fidelity as a probe for a deconfined quantum critical point,” *Phys. Rev. B* **100**, 064427 (2019).
- 69 Brenden Roberts, Shenghan Jiang, and Olexei I. Motrunich, “Deconfined quantum critical point in one dimension,” *Phys. Rev. B* **99**, 165143 (2019).
- 70 Adam Nahum, J. T. Chalker, P. Serna, M. Ortuño, and A. M. Somoza, “Deconfined quantum criticality, scaling violations, and classical loop models,” *Phys. Rev. X* **5**, 041048 (2015).
- 71 Zheng Zhou, Liangdong Hu, W. Zhu, and Yin-Chen He, “The $SO(5)$ deconfined phase transition under the fuzzy sphere microscope: Approximate conformal symmetry, pseudo-criticality, and operator spectrum,” (2023), [arXiv:2306.16435 \[cond-mat.str-el\]](#).
- 72 Yuhai Liu, Zhenjiu Wang, Toshihiro Sato, Martin Hohenadler, Chong Wang, Wenan Guo, and Fakher F Assaad, “Superconductivity from the condensation of topological defects in a quantum spin-hall insulator,” *Nature Communications* **10**, 2658 (2019).
- 73 Jonathan D’Emidio, “Lee-yang zeros at $o(3)$ and deconfined quantum critical points,” (2023), [arXiv:2308.00575 \[cond-mat.str-el\]](#).
- 74 Jonathan D’Emidio and Ribhu K. Kaul, “New easy-plane C_1^{N-1} fixed points,” *Phys. Rev. Lett.* **118**, 187202 (2017).
- 75 Kun Chen, Yuan Huang, Youjin Deng, A. B. Kuklov, N. V. Prokof’ev, and B. V. Svistunov, “Deconfined criticality flow in the heisenberg model with ring-exchange interactions,” *Phys. Rev. Lett.* **110**, 185701 (2013).
- 76 Jing Guo, Guangyu Sun, Bowen Zhao, Ling Wang, Wenshan Hong, Vladimir A. Sidorov, Nvsen Ma, Qi Wu, Shiliang Li, Zi Yang Meng, Anders W. Sandvik, and Liling Sun, “Quantum phases of $\text{SrCu}_2(\text{BO}_3)_2$ from high-pressure thermodynamics,” *Phys. Rev. Lett.* **124**, 206602 (2020).
- 77 Yi Cui, Lu Liu, Huihang Lin, Kai-Hsin Wu, Wenshan Hong, Xuefei Liu, Cong Li, Ze Hu, Ning Xi, Shiliang Li, *et al.*, “Proximate deconfined quantum critical point in $\text{SrCu}_2(\text{BO}_3)_2$,” *Science* **380**, 1179–1184 (2023).
- 78 Tiancheng Song, Yanyu Jia, Guo Yu, Yue Tang, Pengjie Wang, Ratnadwip Singha, Xin Gui, Ayelet J. Uzan, Michael Onyszczyk, Kenji Watanabe, Takashi Taniguchi, Robert J. Cava, Leslie M. Schoop, N. P. Ong, and Sanfeng Wu, “Unconventional superconducting quantum criticality in monolayer WTe_2 ,” (2023), [arXiv:2303.06540 \[cond-mat.mes-hall\]](#).
- 79 M. Saffman, T. G. Walker, and K. Mølmer, “Quantum information with rydberg atoms,” *Rev. Mod. Phys.* **82**, 2313–2363 (2010).
- 80 X.-L. Deng, D. Porras, and J. I. Cirac, “Effective spin quantum phases in systems of trapped ions,” *Phys. Rev. A* **72**, 063407 (2005).
- 81 T Lahaye, C Menotti, L Santos, M Lewenstein, and T Pfau, “The physics of dipolar bosonic quantum gases,” *Reports on Progress in Physics* **72**, 126401 (2009).
- 82 Helmut Ritsch, Peter Domokos, Ferdinand Brennecke, and Tilman Esslinger, “Cold atoms in cavity-generated dynamical optical potentials,” *Rev. Mod. Phys.* **85**, 553–601 (2013).
- 83 Lincoln D Carr, David DeMille, Roman V Krems, and Jun Ye, “Cold and ultracold molecules: science, technology and applications,” *New Journal of Physics* **11**, 055049 (2009).
- 84 Rainer Blatt and Christian F Roos, “Quantum simulations with trapped ions,” *Nature Physics* **8**, 277–284 (2012).
- 85 Joseph W Britton, Brian C Sawyer, Adam C Keith, C-C Joseph Wang, James K Freericks, Hermann Uys, Michael J Biercuk, and John J Bollinger, “Engineered two-dimensional ising interactions in a trapped-ion quantum simulator with hundreds of spins,” *Nature* **484**, 489–492 (2012).
- 86 R Islam, Crystal Senko, Wes C Campbell, S Korenblit, J Smith, A Lee, EE Edwards, C-CJ Wang, JK Freericks, and C Monroe, “Emergence and frustration of magnetism with variable-range interactions in a quantum simulator,” *science* **340**, 583–587 (2013).
- 87 Philip Richerme, Zhe-Xuan Gong, Aaron Lee, Crystal Senko, Jacob Smith, Michael Foss-Feig, Spyridon Michalakis, Alexey V Gorshkov, and Christopher Monroe, “Non-local propagation of correlations in quantum systems with long-range interactions,” *Nature* **511**, 198–201 (2014).
- 88 Petar Jurcevic, Ben P Lanyon, Philipp Hauke, Cornelius Hempel, Peter Zoller, Rainer Blatt, and Christian F Roos, “Quasiparticle engineering and entanglement propagation in a quantum many-body system,” *Nature* **511**, 202–205 (2014).
- 89 Xue-Jia Yu, Sheng Yang, Jing-Bo Xu, and Limei Xu, “Fidelity susceptibility as a diagnostic of the commensurate-incommensurate transition: A revisit of the programmable rydberg chain,” *Phys. Rev. B* **106**, 165124 (2022).
- 90 Nicolò Defenu, Tilman Enss, Michael Kastner, and Giovanna Morigi, “Dynamical critical scaling of long-range interacting quantum magnets,” *Phys. Rev. Lett.* **121**, 240403 (2018).
- 91 Nicolò Defenu, Tobias Donner, Tommaso Macrì, Guido Pagano, Stefano Ruffo, and Andrea Trombettoni, “Long-range interacting quantum systems,” (2021), [arXiv:2109.01063 \[cond-mat.quant-gas\]](#).
- 92 Nicolò Defenu, Alessio Leroose, and Silvia Pappalardi, “Out-of-equilibrium dynamics of quantum many-body systems with long-range interactions,” (2023), [arXiv:2307.04802 \[cond-mat.quant-gas\]](#).
- 93 Marvin Syed, Tilman Enss, and Nicolò Defenu, “Dynamical quantum phase transition in a bosonic system with long-range interactions,” *Phys. Rev. B* **103**, 064306 (2021).
- 94 Nicolò Defenu, Andrea Trombettoni, and Stefano Ruffo, “Anisotropic long-range spin systems,” *Phys. Rev. B* **94**, 224411 (2016).
- 95 Z.-X. Gong, M. F. Maghrebi, A. Hu, M. L. Wall, M. Foss-Feig, and A. V. Gorshkov, “Topological phases with long-range interactions,” *Phys. Rev. B* **93**, 041102 (2016).
- 96 Z.-X. Gong, M. F. Maghrebi, A. Hu, M. Foss-Feig, P. Richerme, C. Monroe, and A. V. Gorshkov, “Kaleidoscope of quantum phases in a long-range interacting spin-1 chain,” *Phys. Rev. B* **93**, 205115 (2016).
- 97 Xiaoyang Shen, “Long range syk model and boundary syk model,” (2023), [arXiv:2308.12598 \[hep-th\]](#).
- 98 Michael E. Fisher, Shang-keng Ma, and B. G. Nickel, “Critical exponents for long-range interactions,” *Phys. Rev. Lett.* **29**, 917–920 (1972).
- 99 Nicolò Defenu, Andrea Trombettoni, and Stefano Ruffo, “Criticality and phase diagram of quantum long-range $o(n)$ models,” *Phys. Rev. B* **96**, 104432 (2017).
- 100 Nicolò Defenu, Alessandro Codello, Stefano Ruffo, and Andrea Trombettoni, “Criticality of spin systems with weak long-range

- interactions,” *Journal of Physics A: Mathematical and Theoretical* **53**, 143001 (2020).
- 101 Guido Giachetti, Nicolò Defenu, Stefano Ruffo, and Andrea Trombettoni, “Berezinskii-kosterlitz-thouless phase transitions with long-range couplings,” *Phys. Rev. Lett.* **127**, 156801 (2021).
 - 102 Guido Giachetti, Andrea Trombettoni, Stefano Ruffo, and Nicolò Defenu, “Berezinskii-kosterlitz-thouless transitions in classical and quantum long-range systems,” *Phys. Rev. B* **106**, 014106 (2022).
 - 103 Alessandro Codello, Nicolò Defenu, and Giulio D’Odorico, “Critical exponents of $\phi(n)$ models in fractional dimensions,” *Phys. Rev. D* **91**, 105003 (2015).
 - 104 Menghan Song, Jiarui Zhao, Chengkang Zhou, and Zi Yang Meng, “Dynamical properties of quantum many-body systems with long range interactions,” (2023), [arXiv:2301.00829 \[cond-mat.str-el\]](#).
 - 105 Menghan Song, Jiarui Zhao, Yang Qi, Junchen Rong, and Zi Yang Meng, “Quantum criticality and entanglement for 2d long-range heisenberg bilayer,” (2023), [arXiv:2306.05465 \[cond-mat.str-el\]](#).
 - 106 Jiarui Zhao, Menghan Song, Yang Qi, Junchen Rong, and Zi Yang Meng, “Finite-temperature critical behaviors in 2d long-range quantum heisenberg model,” (2023), [arXiv:2306.01044 \[cond-mat.str-el\]](#).
 - 107 Nicolò Defenu, Andrea Trombettoni, and Alessandro Codello, “Fixed-point structure and effective fractional dimensionality for $\phi(n)$ models with long-range interactions,” *Phys. Rev. E* **92**, 052113 (2015).
 - 108 Mohammad F. Maghrebi, Zhe-Xuan Gong, Michael Foss-Feig, and Alexey V. Gorshkov, “Causality and quantum criticality in long-range lattice models,” *Phys. Rev. B* **93**, 125128 (2016).
 - 109 Mohammad F. Maghrebi, Zhe-Xuan Gong, and Alexey V. Gorshkov, “Continuous Symmetry Breaking in 1D Long-Range Interacting Quantum Systems,” *Phys. Rev. Lett.* **119**, 023001 (2017).
 - 110 Sibin Yang, Dao-Xin Yao, and Anders W. Sandvik, “Deconfined quantum criticality in spin-1/2 chains with long-range interactions,” (2020), [arXiv:2001.02821 \[physics.comp-ph\]](#).
 - 111 Anders W. Sandvik, “Ground states of a frustrated quantum spin chain with long-range interactions,” *Phys. Rev. Lett.* **104**, 137204 (2010).
 - 112 Xue-Jia Yu, Chengxiang Ding, and Limei Xu, “Quantum criticality of a F_3 -symmetric spin chain with long-range interactions,” *Phys. Rev. E* **107**, 054122 (2023).
 - 113 DinhDuy Vu, Ke Huang, Xiao Li, and S. Das Sarma, “Fermionic many-body localization for random and quasiperiodic systems in the presence of short- and long-range interactions,” *Phys. Rev. Lett.* **128**, 146601 (2022).
 - 114 Jia Ning Leaw, Ho-Kin Tang, Maxim Trushin, Fakhre F. Asaad, and Shaffique Adam, “Universal fermi-surface anisotropy renormalization for interacting dirac fermions with long-range interactions,” *Proceedings of the National Academy of Sciences* **116**, 26431–26434 (2019).
 - 115 Areg Ghazaryan and Tapash Chakraborty, “Long-range coulomb interaction and majorana fermions,” *Phys. Rev. B* **92**, 115138 (2015).
 - 116 Davide Vodola, Luca Lepori, Elisa Ercolessi, Alexey V. Gorshkov, and Guido Pupillo, “Kitaev chains with long-range pairing,” *Phys. Rev. Lett.* **113**, 156402 (2014).
 - 117 Brenden Roberts, Shenghan Jiang, and Olexei I Motrunich, “Deconfined quantum critical point in one dimension,” *Physical Review B* **99**, 165143 (2019).
 - 118 Christopher Mudry, Akira Furusaki, Takahiro Morimoto, and Toshiya Hikihara, “Quantum phase transitions beyond landau-ginzburg theory in one-dimensional space revisited,” *Physical Review B* **99**, 205153 (2019).
 - 119 Rui-Zhen Huang, Da-Chuan Lu, Yi-Zhuang You, Zi Yang Meng, and Tao Xiang, “Emergent symmetry and conserved current at a one-dimensional incarnation of deconfined quantum critical point,” *Physical Review B* **100**, 125137 (2019).
 - 120 Steven R. White, “Density matrix formulation for quantum renormalization groups,” *Phys. Rev. Lett.* **69**, 2863–2866 (1992).
 - 121 U. Schollwöck, “The density-matrix renormalization group,” *Rev. Mod. Phys.* **77**, 259–315 (2005).
 - 122 Ulrich Schollwöck, “The density-matrix renormalization group in the age of matrix product states,” *Annals of Physics* **326**, 96–192 (2011), january 2011 Special Issue.
 - 123 F. Verstraete, D. Porras, and J. I. Cirac, “Density matrix renormalization group and periodic boundary conditions: A quantum information perspective,” *Phys. Rev. Lett.* **93**, 227205 (2004).
 - 124 Goldenfeld Nigel, *Lectures on Phase Transitions and the Renormalization Group*, 1st ed. (CRC Press, 1992).
 - 125 Qiang Luo, Jize Zhao, and Xiaoqun Wang, “Intrinsic jump character of first-order quantum phase transitions,” *Phys. Rev. B* **100**, 121111 (2019).
 - 126 Qiang Luo, Shijie Hu, Jinbin Li, Jize Zhao, Hae-Young Kee, and Xiaoqun Wang, “Spontaneous dimerization, spin-nematic order, and deconfined quantum critical point in a spin-1 kitaev chain with tunable single-ion anisotropy,” *Phys. Rev. B* **107**, 245131 (2023).
 - 127 K. Binder, “Finite size scaling analysis of ising model block distribution functions,” *Z. Physik B - Condensed Matter* **43**, 119–140 (1981).
 - 128 Katharina Vollmayr, Joseph D. Reger, Manfred Scheucher, and Kurt Binder, “Finite size effects at thermally-driven first order phase transitions: A phenomenological theory of the order parameter distribution,” *Z. Physik B - Condensed Matter* **91**, 113–125 (1993).
 - 129 Anders W. Sandvik, “Computational studies of quantum spin systems,” *AIP Conference Proceedings* **1297**, 135–338 (2010).
 - 130 Yan-Cheng Wang, Yang Qi, Shu Chen, and Zi Yang Meng, “Caution on emergent continuous symmetry: A monte carlo investigation of the transverse-field frustrated ising model on the triangular and honeycomb lattices,” *Phys. Rev. B* **96**, 115160 (2017).
 - 131 AB Kuklov, NV Prokof’Ev, BV Svistunov, and Matthias Troyer, “Deconfined criticality, runaway flow in the two-component scalar electrodynamics and weak first-order superfluid-solid transitions,” *Annals of Physics* **321**, 1602–1621 (2006).
 - 132 G. J. Sreejith, Stephen Powell, and Adam Nahum, “Emergent $so(5)$ symmetry at the columnar ordering transition in the classical cubic dimer model,” *Phys. Rev. Lett.* **122**, 080601 (2019).
 - 133 Pablo Serna and Adam Nahum, “Emergence and spontaneous breaking of approximate $O(4)$ symmetry at a weakly first-order deconfined phase transition,” *Phys. Rev. B* **99**, 195110 (2019).
 - 134 Toshihiro Sato, Martin Hohenadler, and Fakhre F. Assaad, “Dirac fermions with competing orders: Non-landau transition with emergent symmetry,” *Phys. Rev. Lett.* **119**, 197203 (2017).
 - 135 Thierry Giamarchi, *Quantum physics in one dimension*, Vol. 121 (Clarendon press, 2003).
 - 136 Chen-Ning Yang and Chen-Ping Yang, “One-dimensional chain of anisotropic spin-spin interactions. i. proof of bethe’s hypothesis for ground state in a finite system,” *Physical Review* **150**, 321 (1966).
 - 137 Chen-Ning Yang and Chen-Ping Yang, “One-dimensional chain of anisotropic spin-spin interactions. ii. properties of the ground-state energy per lattice site for an infinite system,” *Physical Review* **150**, 327 (1966).
 - 138 Chen-Ning Yang and Chen-Ping Yang, “One-dimensional chain

- of anisotropic spin-spin interactions. iii. applications,” *Physical Review* **151**, 258 (1966).
- ¹³⁹ Da-Chuan Lu, Cenke Xu, and Yi-Zhuang You, “Self-duality protected multicriticality in deconfined quantum phase transitions,” *Phys. Rev. B* **104**, 205142 (2021).
- ¹⁴⁰ Bowen Zhao, Phillip Weinberg, and Anders W Sandvik, “Symmetry-enhanced discontinuous phase transition in a two-dimensional quantum magnet,” *Nature Physics* **15**, 678–682 (2019).
- ¹⁴¹ Guangyu Sun, Nvsn Ma, Bowen Zhao, Anders W. Sandvik, and Zi Yang Meng, “Emergent $o(4)$ symmetry at the phase transition from plaquette-singlet to antiferromagnetic order in quasi-two-dimensional quantum magnets*,” *Chinese Physics B* **30**, 067505 (2021).
- ¹⁴² G. J. Sreejith, Stephen Powell, and Adam Nahum, “Emergent $so(5)$ symmetry at the columnar ordering transition in the classical cubic dimer model,” *Phys. Rev. Lett.* **122**, 080601 (2019).
- ¹⁴³ Pablo Serna and Adam Nahum, “Emergence and spontaneous breaking of approximate $O(4)$ symmetry at a weakly first-order deconfined phase transition,” *Phys. Rev. B* **99**, 195110 (2019).
- ¹⁴⁴ Julia Wildeboer, Nisheeta Desai, Jonathan D’Emidio, and Ribhu K. Kaul, “First-order néel to columnar valence bond solid transition in a model square-lattice $s = 1$ antiferromagnet,” *Phys. Rev. B* **101**, 045111 (2020).
- ¹⁴⁵ Julia Wildeboer, Nisheeta Desai, Jonathan D’Emidio, and Ribhu K. Kaul, “First-order néel to columnar valence bond solid transition in a model square-lattice $s = 1$ antiferromagnet,” *Phys. Rev. B* **101**, 045111 (2020).
- ¹⁴⁶ Jiabin Yu, Radu Roiban, Shao-Kai Jian, and Chao-Xing Liu, “Finite-scale emergence of 2 + 1D supersymmetry at first-order quantum phase transition,” *Phys. Rev. B* **100**, 075153 (2019).
- ¹⁴⁷ Jong Yeon Lee, Joshua Ramette, Max A. Metlitski, Vladan Vuletic, Wen Wei Ho, and Soonwon Choi, “Landau-forbidden quantum criticality in rydberg quantum simulators,” (2022), [arXiv:2207.08829 \[cond-mat.str-el\]](https://arxiv.org/abs/2207.08829).
- ¹⁴⁸ Chi-Ming Chang, Ying-Hsuan Lin, Shu-Heng Shao, Yifan Wang, and Xi Yin, “Topological defect lines and renormalization group flows in two dimensions,” *Journal of High Energy Physics* **2019**, 1–85 (2019).
- ¹⁴⁹ Ryan Thorngren and Yifan Wang, “Fusion category symmetry ii: categoriosities at $c = 1$ and beyond,” *arXiv preprint arXiv:2106.12577* (2021).
- ¹⁵⁰ Matthew Fishman, Steven R. White, and E. Miles Stoudenmire, “The ITensor Software Library for Tensor Network Calculations,” *SciPost Phys. Codebases*, 4 (2022).

Appendix A: EFFECTIVE THEORY FOR THE 1D SPIN CHAIN WITH SHORT-RANGE INTERACTION

In this appendix, we summary the basic effective continuum theory description of the generalized 1D spin-1/2 chain, JM model^{15,117–119},

$$H = \frac{1}{4} \sum_j \left(-J_x \sigma_j^x \sigma_{j+1}^x - J_z \sigma_j^z \sigma_{j+1}^z \right) + \frac{1}{4} \sum_j \left(+K_x \sigma_j^x \sigma_{j+2}^x + K_z \sigma_j^z \sigma_{j+2}^z \right) \quad (A1)$$

where the spin operators have been represented by Pauli matrices $\mathbf{S}_j = \frac{1}{2} \boldsymbol{\sigma}_j = \frac{1}{2} (\sigma_j^x, \sigma_j^y, \sigma_j^z)$. The effective field theory could be obtained from Bosonization approach based on the transformation^{15,118,135},

$$\sigma_j^y \sim \frac{2}{\pi} (\theta_{j+1/2} - \theta_{j-1/2}), \quad \sigma_j^z \sim \cos(\phi_j), \quad \sigma_j^x \sim -\sin(\phi_j), \quad [\theta_{j+1/2}, \phi_{j'}] = i\pi \Theta(j + 1/2 - j'), \quad (A2)$$

where θ and ϕ is a pair of conjugate field, $\Theta(x)$ is a Heaviside step function. Taking continuum limit, the effective action in the imaginary-time path integral formulation is given by¹⁵,

$$S[\phi, \theta] = \int d\tau dx \left[\frac{i}{\pi} \partial_\tau \phi \partial_x \theta + \frac{v}{2\pi} \left(\frac{1}{g} (\partial_x \theta)^2 + g (\partial_x \phi)^2 \right) \right] + \int d\tau dx \left[\lambda_u \cos(4\theta) + \lambda_a \cos(2\phi) \right]. \quad (A3)$$

where τ is the imaginary time, x is the spatial coordinate, v is the velocity and g is the Luttinger parameter. λ_u and λ_a terms are the most relevant operators which have the largest scaling dimension and reflect the symmetries of the system. They will drive the possible transition to the ordered phase, reflecting by the pinning of the (θ, ϕ) fields. In the continuum theory, the order parameters for the z -FM phase and VBS phase are represented by the continuous bosonic fields,

$$\Psi_{z\text{FM}} \sim \cos(\phi), \quad \Psi_{\text{VBS}} \sim \cos(2\theta).$$

The z -FM state $\Psi_{z\text{FM}}$ is invariant under the lattice translational symmetry $T_x(\phi, \theta) \rightarrow (\phi, \theta + \pi/2)$ and \mathbb{Z}_2^z spin rotation symmetry around z -axis $g_z(\phi, \theta) \rightarrow (-\phi, -\theta)$, but breaks the \mathbb{Z}_2^x spin rotation symmetry around x -axis $g_x(\phi, \theta) \rightarrow (-\phi + \pi, -\theta)$ and time-reversal symmetry $\mathcal{T}(\phi, \theta, i) \rightarrow (\phi + \pi, -\theta, -i)$. The VBS state Ψ_{VBS} is invariant under g_x, g_z and \mathcal{T} , but breaks T_x . The tree-level scalings of the cos-operators are given by $\dim[\cos(2n\theta)] = n^2 g$ and $\dim[\cos(m\phi)] = \frac{m^2}{4g}$. The tree-level β -functions for the short-ranged λ_u - and λ_a -term are given by,

$$\frac{d\lambda_u}{dl} = \left(2 - \dim[\cos(4\theta)] \right) \lambda_u = (2 - 4g) \lambda_u, \quad \frac{d\lambda_a}{dl} = \left(2 - \dim[\cos(2\phi)] \right) \lambda_a = \left(2 - \frac{1}{g} \right) \lambda_a. \quad (A4)$$

The scaling behaviors of the z -FM correlation and VBS correlation are given by

$$\langle \Psi_{z\text{FM}}(r) \Psi_{z\text{FM}}(0) \rangle \sim \frac{1}{r^{1/2g}}, \quad \langle \Psi_{\text{VBS}}(r) \Psi_{\text{VBS}}(0) \rangle \sim \frac{1}{r^{2g}}$$

However, such continuum theory is not complete for the understanding of deconfined quantum critical point between z -FM and VBS order, and a dual theory is necessary to fully characterize the critical behavior¹⁵.

a. Dual Luttinger-like theory To describe the deconfined quantum phase transition between z -FM and VBS order, it is more sufficient to work in the duality formulation, which is also represented by a Luttinger-like theory^{15,117},

$$S[\tilde{\phi}, \tilde{\theta}] = \int d\tau dx \left[\frac{i}{\pi} \partial_\tau \tilde{\phi} \partial_x \tilde{\theta} + \frac{\tilde{v}}{2\pi} \left(\frac{1}{\tilde{g}} (\partial_x \tilde{\theta})^2 + \tilde{g} (\partial_x \tilde{\phi})^2 \right) \right] + \int d\tau dx \left[\lambda \cos(2\tilde{\theta}) + \lambda' \cos(4\tilde{\theta}) + \kappa \cos(4\tilde{\phi}) \right] \quad (\text{A5})$$

where $\tilde{\phi}$ and $\tilde{\theta}$ are a pair of conjugate fields in the dual theory, \tilde{v} and \tilde{g} are corresponding velocity and Luttinger parameter. λ, λ' and κ are several lowest-order short-range interactions.

The phase transition between z -FM and VBS order lies within the regime $\tilde{g} \in (1/2, 2)$ such that λ -term is the single relevant operator which drives the phase transition happens when its sign alters. The correlation length exponent at the critical point follows the scaling dimension of $\lambda \cos(2\tilde{\theta})$, that is¹⁵,

$$\nu^{-1} = 2 - \dim[\cos(2\tilde{\theta})] = 2 - \tilde{g}, \quad \nu = \frac{1}{2 - \tilde{g}}.$$

In this dual Luttinger-like theory, the order parameters for the z -FM and VBS phase are decoded into a compatible form based on a single field $\tilde{\theta}$

$$\Psi_{z\text{FM}} \sim \sin(\tilde{\theta}), \quad \Psi_{\text{VBS}} \sim \cos(\tilde{\theta}), \quad (\text{A6})$$

which, of course, have the same scaling dimension $\dim[\Psi_{z\text{FM}}] = \dim[\Psi_{\text{VBS}}] = \tilde{g}/4$ and similar correlation behavior at the critical point,

$$\langle \Psi_{z\text{FM}}(r) \Psi_{z\text{FM}}(0) \rangle \sim \frac{1}{r^{2\dim\Psi_{z\text{FM}}}} = \frac{1}{r^{\tilde{g}/2}}, \quad \langle \Psi_{\text{VBS}}(r) \Psi_{\text{VBS}}(0) \rangle \sim \frac{1}{r^{2\dim\Psi_{\text{VBS}}}} = \frac{1}{r^{\tilde{g}/2}}.$$

The phase transition between z -FM and VBS phase is tuned by λ , while at the critical point $\lambda = 0$ there exist an emergent $O(2)$ symmetry corresponding to $\tilde{\theta}$ part.

Appendix B: DETAILS OF RENORMALIZATION GROUP CALCULATIONS FOR THE LONG-RANGE SINE-GORDON MODEL

In this work, we consider the long-range interaction Hamiltonian,

$$H_{LRP} = \sum_i (-J_z S_i^z S_{i+1}^z + K_x S_i^x S_{i+2}^x + K_z S_i^z S_{i+2}^z) - \frac{J_z}{N(\alpha)} \sum_{i,j} \frac{S_i^z S_j^z}{|i-j|^\alpha}, \quad (\text{A1})$$

where J is the interaction strength, parameter α tunes the power of long-range interactions. $N(\alpha) (= \frac{1}{N-1} \sum_{i \neq j} \frac{1}{|i-j|^\alpha})$ is the Kac factor to preserve the Hamiltonian extensive. To connect this model with the known short-range model (A1), we can separated the long-range term in the form,

$$-\frac{J_z}{N(\alpha)} \sum_{i,j} \frac{S_i^z S_j^z}{|i-j|^\alpha} = -\frac{J_z}{N(\alpha)} \sum_{|i-j|=1} S_i^z S_j^z - \frac{J_z}{N(\alpha)} \sum_{|i-j|>1} \frac{S_i^z S_j^z}{|i-j|^\alpha} = -J'_z \sum_i S_i^z S_{i+1}^z - \frac{J_z}{N(\alpha)} \sum_{|i-j|>1} \frac{S_i^z S_j^z}{|i-j|^\alpha}.$$

Here the first term is just the conventional nearest-neighbor coupling. We consider the effective continuum theory for the long-range interactions,

$$\begin{aligned} H_{LR} &= - \sum_{i,j} \frac{J_L}{|i-j|^\alpha} \sigma_i^z \sigma_j^z = - \sum_{i,j} \frac{J_L}{|i-j|^\alpha} \cos \phi_i \cos \phi_j \rightarrow - \int dx dx' \frac{J_L}{|x-x'|^\alpha} \cos \phi(x) \cos \phi(x') \\ &\rightarrow - \frac{1}{2} \int dx dr \frac{J_L}{|r|^\alpha} \left(\cos [\phi(x+r) - \phi(x)] + \cos [\phi(x+r) + \phi(x)] \right) \end{aligned} \quad (\text{A2})$$

Expand the first term for small r , we can obtain

$$\frac{1}{2} \int dx dr \frac{J_L}{|r|^\alpha} \cos [\phi(x+r) - \phi(x)] \approx \frac{1}{2} \int dx dr \frac{J_L}{|r|^\alpha} \left(1 - \frac{1}{2} (r \nabla \phi)^2\right)$$

which only normalize the Luttinger parameters. In general, long-range correlated interaction part of the action is given by,

$$S_{LR} = \frac{1}{2} \int d\tau \int dx dr \frac{1}{|r|^\alpha} \left(\lambda_+ \cos [\phi(x+r, \tau) + \phi(x, \tau)] + \lambda_- \cos [\phi(x+r, \tau) - \phi(x, \tau)] \right)$$

with the bare interaction strength $\lambda_+ < 0$ and $\lambda_- < 0$.

For the effective Bosonization theory, we follow the conventional tree-level RG analysis of the sine-Gordon model¹³⁵. Separating the field into slow and fast modes ($\phi = \phi_< + \phi_>$ and $\phi = \theta_< + \theta_>$) and integrating over the fast mode ($\phi_>, \theta_>$), the partition function can be expanded in the form,

$$Z = \int D\phi D\theta e^{-S_0 - S_1} = \int D\phi_< D\theta_< \int D\phi_> D\theta_> e^{-S_0, < - S_0, > - S_1} = \int D\phi_< D\theta_< e^{-S_0, <} \sum_{n=0}^{\infty} \frac{1}{n!} \langle (-S_1)^n \rangle_>$$

where the integral of fast mode gives the average,

$$\langle \dots \rangle_> \equiv \int D\phi_> D\theta_> e^{-S_0, >} (\dots).$$

The effective action under the renormalization is,

$$S_{eff} = S_{0, <} + \langle S_1 \rangle_> - \frac{1}{2} \langle S_1^2 \rangle_{>, c}. \quad (A3)$$

The tree-level scalings of the operators can be obtained from the first order term $\langle S_1 \rangle_>$. We consider the tree-level scaling for the long-range correlated terms,

$$\begin{aligned} S_\sigma &= \frac{1}{2} \lambda_\sigma \int d\tau \int dx dr \frac{1}{|r|^\alpha} \cos [\phi(x+r, \tau) + \sigma \phi(x, \tau)] \equiv \frac{1}{2} \lambda_\sigma \int d\tau \int dx dr \frac{1}{|r|^\alpha} \cos [\Delta_r^\sigma \phi] \\ &= \frac{1}{2} \lambda_\sigma \int d\tau \int dx dr \frac{1}{|r|^\alpha} \cos [\Delta_r^\sigma \phi_< + \Delta_r^\sigma \phi_>] \end{aligned}$$

Integrating out the fast mode, the lowest order correction is

$$\langle S_\sigma \rangle_> = \frac{1}{2} \lambda_\sigma \int d\tau \int dx dr \frac{1}{|r|^\alpha} \cos [\Delta_r^\sigma \phi_<] \langle \cos [\Delta_r^\sigma \phi_>] \rangle_>$$

Here, the renormalization gives the contribution,

$$\begin{aligned} \langle \cos [\Delta_r^\sigma \phi_>] \rangle_> &= \exp \left(- \frac{1}{2} \langle [\Delta_r^\sigma \phi_>]^2 \rangle_> \right) = \exp \left(- \frac{1}{2} \langle [\phi(x+r, \tau) + \sigma \phi(x, \tau)]^2 \rangle_> \right) \\ &= \exp \left(- \frac{1}{2} \langle [\phi(r, 0) + \sigma \phi(0)]^2 \rangle_> \right) \end{aligned}$$

where the correlation function of $\phi(r)$ field can be calculated out directly,

$$\frac{1}{2} \langle [\phi(r, 0) + \sigma \phi(0)]^2 \rangle_> = \frac{1}{2} \int_{>} \frac{d\omega dq}{(2\pi)^2} (2 + 2\sigma \cos(|qr|)) \frac{v}{g} \frac{\pi}{v^2 q^2 + \omega^2} = \frac{1}{2g} \left(1 + \sigma \cos(|\Lambda r|) \right) \frac{d\Lambda}{\Lambda}$$

The lowest order correction is

$$\langle S_\sigma \rangle_> = \frac{1}{2} \lambda_\sigma \int d\tau \int dx dr \frac{1}{|r|^\alpha} \cos [\Delta_r^\sigma \phi_<] \exp \left(- \frac{1}{2g} \left(1 + \sigma \cos(|\Lambda r|) \right) \frac{d\Lambda}{\Lambda} \right).$$

Up to tree-level, the effective action under renormalization is $S_{\sigma, eff} = S_{\sigma, <} + \langle S_\sigma \rangle_>$. Under the rescaling transformation,

$$\tau \rightarrow e^{dl} \tau, \quad x \rightarrow e^{dl} x, \quad r \rightarrow e^{dl} r, \quad \Lambda \rightarrow e^{-dl} \Lambda,$$

the effective action becomes,

$$\begin{aligned} S_{\sigma,eff} &\rightarrow \frac{1}{2} \lambda_{\sigma} e^{(3-\alpha)dl} \int d\tau \int dx dr \frac{1}{|r|^{\alpha}} \cos [\Delta_r^{\sigma} \phi] \left(1 - \frac{1}{2g} dl - \frac{\sigma}{2g} \cos(|\Lambda r|) dl \right) \\ &= \frac{1}{2} \lambda_{\sigma} \int d\tau \int dx dr \frac{1}{|r|^{\alpha}} \cos [\Delta_r^{\sigma} \phi] \left(1 + (3 - \alpha - \frac{1}{2g}) dl - \frac{\sigma}{2g} \cos(|\Lambda r|) dl \right) \end{aligned}$$

and the RG functional equations for λ_{σ} are

$$\frac{d\lambda_{\sigma}(r)}{dl} = \left(3 - \alpha - \frac{1 + \sigma \cos(|\Lambda r|)}{2g} \right) \lambda_{\sigma}(r).$$

Here, the effective coupling has non-trivial dependence on the momentum cutoff Λ . In the lattice formulation, the coordinates of the system are represented by $r = r_n = na$ ($n = 0, 1, \dots, N-1$), where a is the lattice constant and the total lattice size is $L = Na$. The corresponding discrete set of momentum is $k = k_m = m \frac{\pi}{L} = m \frac{\pi}{Na}$ with $-\frac{N}{2} + 1, \dots, \frac{N}{2}$. In the infrared (long-length) limit, the momentum will flow to the shortest momentum scale $\sim \pi/L$. For smaller r , the oscillation factor $\cos(|\Lambda r|)$ becomes nearly unity, and we can approximately obtain

$$r < r_c : \quad \frac{d\lambda_{\sigma}(r)}{dl} = \left(3 - \alpha - \frac{1 + \sigma}{2g} \right) \lambda_{\sigma}(r).$$

For larger r , the scaling dimension of λ_{-} is bigger than λ_{+} . λ_{-} is more relevant than λ_{+} in general. There exists a critical power α_c below which λ_{σ} becomes most relevant, dominating the physical behavior of the system.

a. long-range interaction in the dual theory We now transform to the effect of long-range interaction in the dual theory. From the representation of the order parameter in Eq. (A6), the long-range interaction in the continuous dual theory is given by,

$$\begin{aligned} S_{LR} &= \int d\tau \int dx dr \frac{\tilde{\lambda}}{|r|^{\alpha}} \sin [\tilde{\theta}(x+r, \tau)] \sin [\tilde{\theta}(x, \tau)] \\ &= \frac{1}{2} \int d\tau \int dx dr \frac{1}{|r|^{\alpha}} \left(\tilde{\lambda}_{-} \cos [\tilde{\theta}(x+r, \tau) - \tilde{\theta}(x, \tau)] - \tilde{\lambda}_{+} \cos [\tilde{\theta}(x+r, \tau) + \tilde{\theta}(x, \tau)] \right). \end{aligned}$$

The renormalization of $\tilde{\lambda}_{\pm}$ takes same form as λ_{\pm} , only taking the substitution $g \rightarrow 1/\tilde{g}$,

$$\frac{d\tilde{\lambda}_{\sigma}(r)}{dl} = \left(3 - \alpha - \tilde{g} \frac{1 + \sigma \cos(|\Lambda r|)}{2} \right) \tilde{\lambda}_{\sigma}(r).$$

Similarly as before, long-range $\tilde{\lambda}_{-}$ interaction will dominate the system when the power smaller than some critical value, $\alpha < \alpha_c$. The scaling dimension of $\tilde{\lambda}_{-}$ is approximately given by

$$\dim[\tilde{\lambda}_{-}] = 3 - \alpha - \tilde{g} \frac{1 - \delta}{2}.$$

with some constant δ . Compare the scaling dimension the long-range $\tilde{\lambda}_{-}$ and short-range interaction λ at the tree-level, we can obtain the critical power α_c ,

$$3 - \alpha - \tilde{g} \frac{1 - \delta}{2} = 2 - \tilde{g}, \quad \rightarrow \quad \alpha_c = 1 + \frac{\tilde{g}}{2}(\delta + 1).$$

The true critical power could lie between $1 + \frac{\tilde{g}}{2} < \alpha_c < 1 + \tilde{g}$.

Appendix C: ADDITIONAL DATA FOR z FM BINDER RATIO AND THE RATIO OF SQUARED ORDER PARAMETERS

In this section, we provide additional results of the z FM Binder ratio U_{zFM} and the ratio of squared order parameters R_2 for other α values.

In Fig. A1, we first present U_{zFM} as a function of J_z for various system sizes at other representative α values. The distinct behaviours of U_{zFM} for $\alpha > \alpha_c$ or $\alpha < \alpha_c$ indicate a fundamentally change of the transition nature as explained in the main text. An extrapolation of the crossing points of U_{zFM} , according to the relation $J_z^*(L) = J_z^c + aL^{-b}$ where $J_z^*(L)$ is the crossing point of $U_{zFM}(L)$ and $U_{zFM}(L+32)$, is also performed to determine the precise boundary between the ordered phases (see Fig. A3). The obtained critical points are then used to complete the ground-state phase diagram displayed in the main text (see Fig. 1).

On the other hand, the ratio of squared order parameters R_2 versus J_z is also analyzed in Fig. A2 for other α values. It is clear that all the curves of different L intersect almost at a single point, which means that R_2 becomes universal at the critical point. The result can be a supportive evidence for the $O(2) \times O(2)$ symmetry appeared along the whole transition line (the dashed line in Fig. 1). Furthermore, a similar extrapolation of the R_2 crossing points is also exhibited in Fig. A3, from which we can see that the extrapolated critical points are consistent with the ones extracted from U_{zFM} quite well.

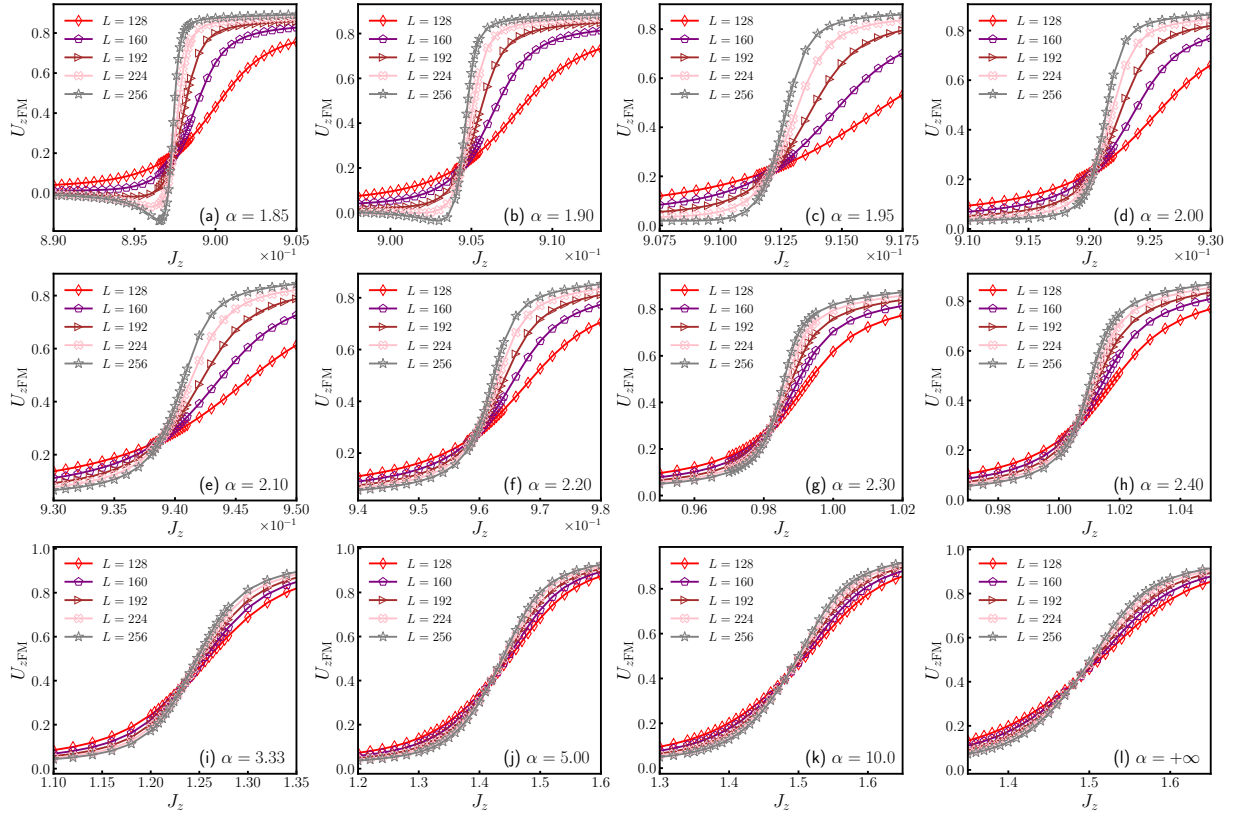


FIG. A1. The Binder ratio of the $z\text{FM}$ order as a function of J_z for (a) $\alpha = 1.85$, (b) $\alpha = 1.90$, (c) $\alpha = 1.95$, (d) $\alpha = 2.00$, (e) $\alpha = 2.10$, (f) $\alpha = 2.20$, (g) $\alpha = 2.30$, (h) $\alpha = 2.40$, (i) $\alpha = 3.33$, (j) $\alpha = 5.00$, (k) $\alpha = 10.0$, and (l) $\alpha = +\infty$.

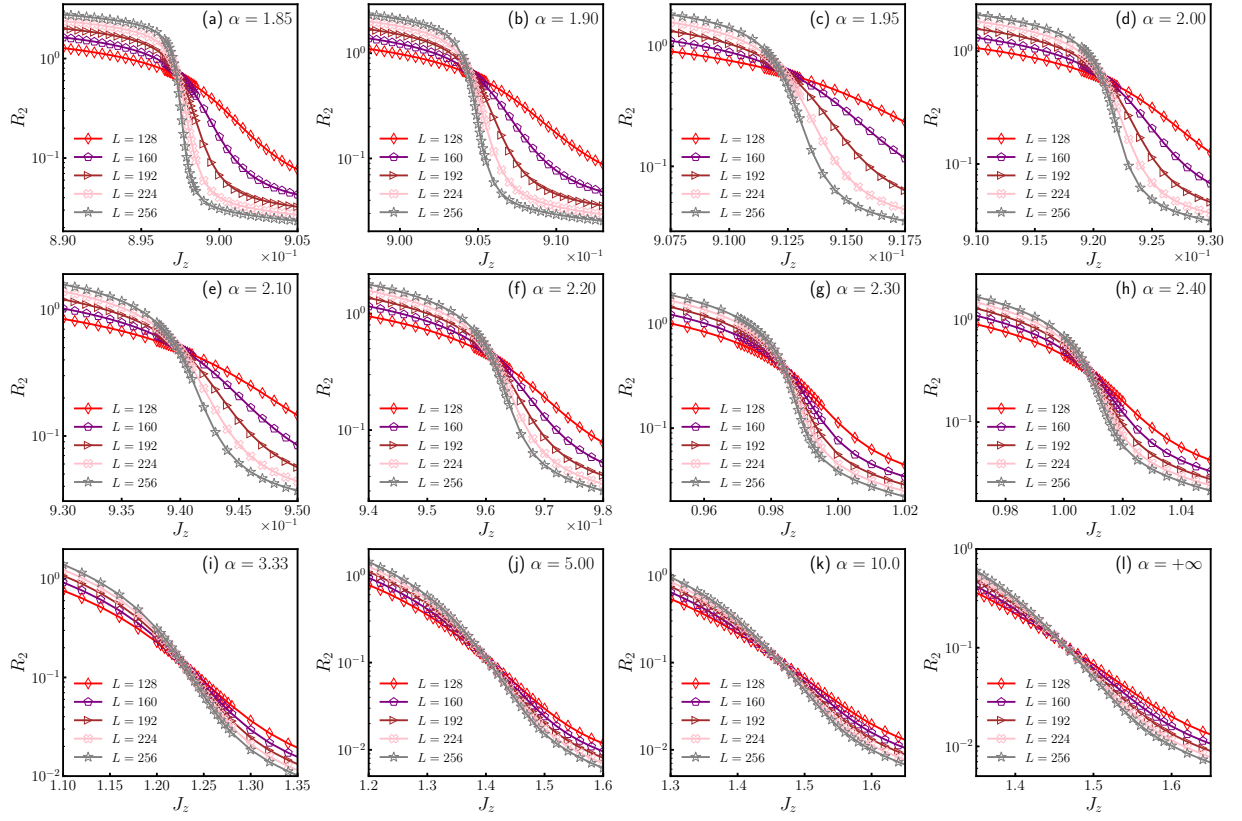


FIG. A2. The ratio of the squared order parameters R_2 as a function of J_z for (a) $\alpha = 1.85$, (b) $\alpha = 1.90$, (c) $\alpha = 1.95$, (d) $\alpha = 2.00$, (e) $\alpha = 2.10$, (f) $\alpha = 2.20$, (g) $\alpha = 2.30$, (h) $\alpha = 2.40$, (i) $\alpha = 3.33$, (j) $\alpha = 5.00$, (k) $\alpha = 10.0$, and (l) $\alpha = +\infty$.

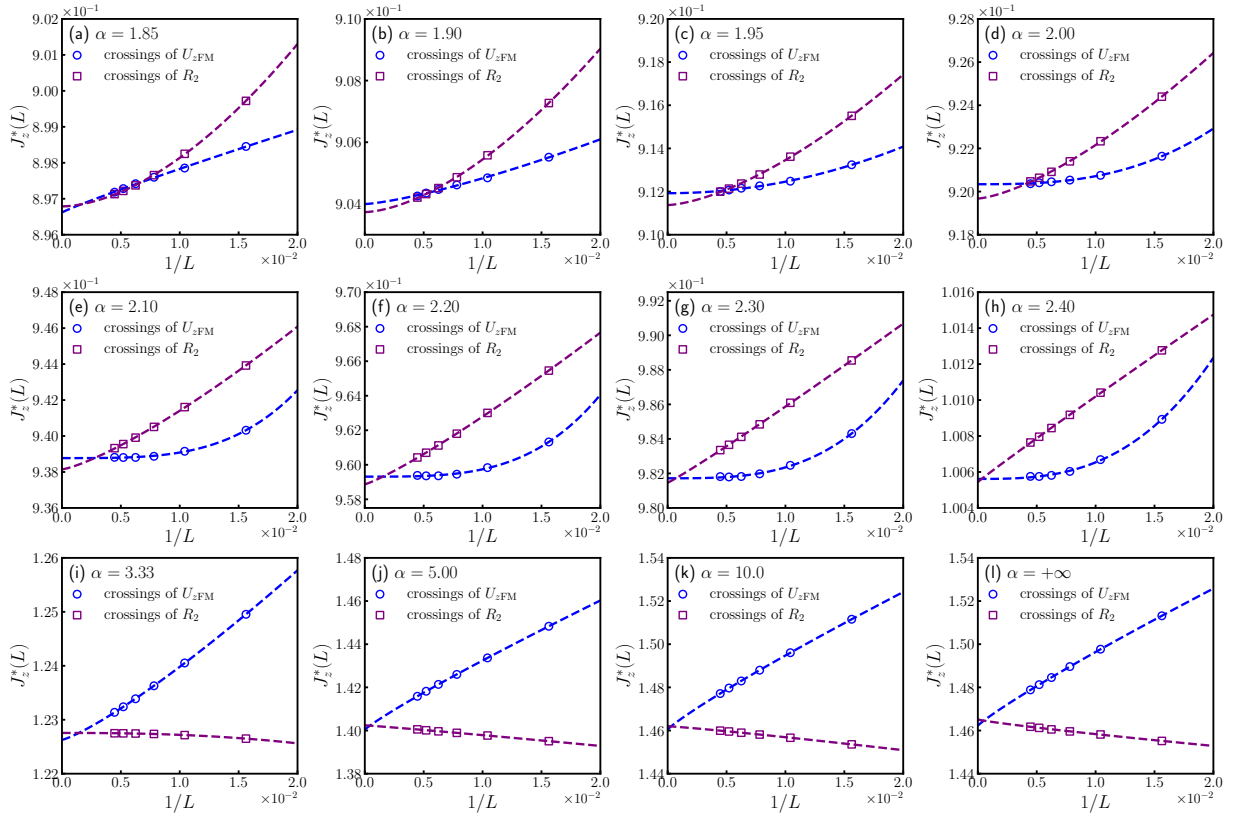


FIG. A3. The crossing locations $J_z^*(L)$ of $U_{z\text{FM}}(L)$ [$R_2(L)$] and $U_{z\text{FM}}(L+32)$ [$R_2(L+32)$] are shown versus $1/L$ for (a) $\alpha = 1.85$, (b) $\alpha = 1.90$, (c) $\alpha = 1.95$, (d) $\alpha = 2.00$, (e) $\alpha = 2.10$, (f) $\alpha = 2.20$, (g) $\alpha = 2.30$, (h) $\alpha = 2.40$, (i) $\alpha = 3.33$, (j) $\alpha = 5.00$, (k) $\alpha = 10.0$, and (l) $\alpha = +\infty$. The curves are least-squares fits according to $J_z^*(L) = J_z^c + aL^{-b}$. The critical points obtained respectively from $U_{z\text{FM}}$ and R_2 are consistent with each other within numerical accuracy.